DEMOCRATIC AND POPULAR REPUBLIC OF ALGERIA

Ministry of High Education and Scientific Research

University of Sciences and Technology Houari Boumediene

Faculty of Mechanical Engineering and Engineering Processes

THESIS

Submitted in partial fulfillment of the requirement of

MAGISTER

In

MECHANICAL ENGINEERING

Mechanical Energy and Porous Media

BY : HAMMOUDI Djamel

Subject

Condensation of vapor in presence of a noncondensable gas though a vertical channel

Publicly defended, on March 10,2016, before the jury:

Mr	A. BOUMEDIEN	Professor, USTHB	President
Mr	A. BENABDESSELAM	Associate Professor, USTHB	Supervisor
Mr	A. AZZI	Professor, USTHB	Examiner
Mr	B.MADANI	Professor, USTHB	Examiner
Mr	A.HADJADJ	Associate Professor, UMBB	Examiner

2015/2016

Abstract

In this work, we present a numerical solution of governing equations for steam condensation in vertical channel in the presence of a noncondensable gas for forced convection. A laminar downward flow of humid air circulates through the channel with a constant temperature and concentration and a uniform profile of velocity at the inlet. The one-third law is adopted to calculate the Thermophysical properties in this study. The mathematical model solution is based on finite volume method and the pressure-velocity coupling is treated by SIMPLER Algorithm. Besides the transverse diffusion, the model includes the axial diffusion. The aim of this work is to carry out an investigation about the condensed flow rate. A wide range of inlet input parameters for the mixture of steam-air has been used to study the heat and mass transfer, where the condensed flow rate has been evaluated for different values of inlet parameters such us the temperature, the Reynolds number and the relative humidity as well as the aspect ratio. The obtained results show that the increase of inlet humidity, inlet Reynolds number and inlet temperature as well as the aspect ratio promotes condensation. The aforementioned parameters have the same effect on the released latent heat for condensation case.

Keywords : Condensation, noncondensable gas, thin liquid film, water vapor-air mixture, forced convection.

<div dir="rtl">

ملخص

الدراسة المتناولة في هذا البحث تقدم الحل الرقمي للمعادلات التي تحكم تكثيف البخار مع وجود غير مكثف في قناة عمودية في حالة الحمل الحراري القسري. تم تطبيق انسياب نزولي صفحي للهواء الرطب داخل القناة مع درجة حرارة, تركيز و سرعة ثابتين عند المدخل. قمنا المنتهية مع معالجة باستخدام قاعدة الثلث لحساب الخصائص الفيزيوحرارية. يستند حل النموذج الرياضي المستعمل على طريقة الأحجام اقتران سرعة-ضغط بواسطة خوارزمية SIMPLER. بالإضافة إلى الإنتشار العرضي, فإن النموذج يتضمن الإنتشار المحوري. الهدف من هذه الدراسة هو حساب التدفق المتكثف. وقد تم استخدام مجموعة واسعة من المقاييس عند مدخل القناة من أجل دراسة الإنتقال الحراري و الكتلي أين تم تقييم التدفق المتكثف بدلالة درجة الحرارة, عدد رينولدز و الرطوبة النسبية عند المدخل بالإضافة إلى عامل الشكل. أظهرت النتائج أن زيادة الرطوبة النسبية, عدد رينولدز و درجة الحرارة عند مدخل القناة بالإضافة إلى عامل الشكل تحسن التكثيف. هذه المعايير لها نفس التأثير على الحرارة الكامنة المتحررة في حالة التكثيف.

كلمات مفتاحيةً: تكثيف، غاز غير مكثف، غشاء سائل رقيق، خليط بخار-غاز، حمل حراري قسري.

</div>

Résumé

Dans ce travail, on présente une résolution numérique des équations gouvernantes pour la condensation d'une vapeur en présence d'un incondensable dans un canal vertical pour le cas de convection forcée. Un écoulement d'air humide laminaire descendant circule dans le canal avec une température, une concentration constantes et un profil de vitesse uniforme à l'entrée. La loi de tiers est adoptée pour calculer les propriétés thermo-physiques. La résolution du modèle mathématique est basée sur la méthode des volumes finis et le couplage vitesse-pression est traité par l'algorithme SIMPLER. En outre de la diffusion transversale, le model inclus la diffusion axial. L'objective de ce travail est d'effectuer une investigation sur le débit condensé. Une large gamme des paramètres d'entrée a été utilisée pour étudier le transfert de chaleur et de masse où le débit condensé a été évalué en fonction des paramètres d'entré tel-que la température, le nombre de Reynolds et l'humidité relative et aussi le facteur de forme. Les résultats obtenus montrent que l'augmentation de l'humidité relative, le nombre de Reynolds et la température à l'entrée du canal et aussi le facteur de forme améliore la condensation. Ces paramètres ont le même effet sur la chaleur latente libérée pour le cas de condensation.

Mots clés : Condensation, gaz incondensable, film liquide mince, mélange vapeur-air, convection forcée.

Dedication

To my family and my friends for everything they have done for me

Acknowledgements

All the praises and deepest gratitude to Allah Almighty, the Omnipotent and the Benevolent, Who has bestowed upon me the quest for knowledge and granted un-flinching determination to complete this work successfully.

*I would like to express my utmost respect and sincere gratitude to my supervisor **Mr. A. BEN ABDESSELAM** for giving me the guidance and motivation that was needed to lead me in the correct direction.*

*I am deeply grateful to all the members of the jury, **Pr. A. BOUMEDIEN**, **Pr. A. AZZI, Pr. B.MADANI** and **Mr. A. HADJADJ** for having accepted to assess my modest work.*

*I owe my deepest gratitude to the head of the "Laboratory of Multiphase Transport and Porous Media" **Pr. K. BOUHADEF**, for welcoming me and providing her full support during my Magister.*

I am also grateful to my English teacher Mrs. OUYED for her help and encouragement.

I extend my sincere thanks to all members of the "Laboratory of Multiphase Transport and Porous Media" for keeping the working environment very nice and friendly.

I am extremely thankful to all my friends and colleagues (Reda, Younes, Youcef, Tarik, Houssam, Sayed, Djamel, Aguelid ...) for their friendship, support and encouragement.

Last but not least, I would like to thank my family members who never failed to give me support and encouragement and who have been there for me.

Contents

CHAPTER V: GENERAL CONCLUSION AND PERSPECTIVE

List of Figures

List of Tables

List of symbols

Nomenclature

C	dimensionless mass fraction $\frac{W-W_{in}}{W_w-W_{in}}$
C_p	specific heat [J/kg·K]
D	diffusion coefficient [m²/s]
D_h	hydraulic diameter,=4 H [m]
f	friction coefficient
g	gravitational acceleration = 9.81 [m/s²]
H	half-distance between the plates [m]
h_{fg}	latent heat of vaporization [kJ/kg]
L	channel length [m]
k	thermal conductivity [W/m·K]
ṁ	condensed mass flow rate per unit width [kg/m.s]
M	molecular weight [g/mol]
Nu_L	latent Nusselt number
Nu_s	sensible Nusselt number
P	pressure [Pa]
Pr	Prandtl number
Re	Reynolds number
S	general source term
Sc	Schmidt number
Sh	Sherwood number
T	temperature [°C or K]
u	axial velocity [m/s]
U	dimensionless axial velocity [m/s]
v	transverse velocity [m/s]
V	dimensionless transverse velocity

V_e	dimensionless condensation or evaporation velocity
W	mass fraction [(g of vapor / kg humid air)]
x	axial coordinate [m]
X	dimensionless axial coordinate
y	transverse coordinate [m]
Y	dimensionless transverse coordinate

Subscripts

a	air
adia	value at the adiabatic wall
in	inlet
L	latent
m	average
ref	refrence
w	value at the isothermal wall
s	sensible
v	vapor

Superscripts

| n | previous iteration |
| n+1 | current iteration |

Greek Symbols

α	thermal diffusion coefficient [m²/s]
γ	aspect ratio
θ	dimensionless temperature
ν	cinematic viscosity [m²/s]
φ	air relative humidity (%)
Φ	general dependent variable
Γ	general diffusion coefficient
δ	film thickness

Acronyms

CFD   computational fluid dynamics

HTC   heat transfer coefficient

NC   noncondensable

GENERAL INTRODUCTION

Condensation of vapor in the presence of noncondensable gases is of great importance in diverse fields of engineering such refrigeration, air cleaning and conditioning systems, humidity control systems, thermal power plant, chemical process industries, because of the great influence of presence of the noncondensable gases on the condensation rate and the heat transfer.

Condensation is the heat transfer process by which a saturated vapor is converted into a liquid by means of removing the latent heat of condensation. The study of this phenomenon becomes a fundamental theme in heat and mass transfer. However, its complexity arises out from the simultaneous intervention of several factors:

- Different types of condensation: fog, droplet or film-wise condensation.
- The flow regimes: laminar, wavy or turbulent, for forced, mixed or natural convection.

- Fluid state: pure or saturated vapor, vapor mixture or vapor-noncondensable gas mixture.
- The influence of several parameters such as the velocity, the pressure, the temperature of the fluids and the walls.
- The geometrical form of condensation devices: vertical, horizontal or inclined plate, tubes.

The condensation process has been studied since 1916, when Nusselt developed an analytical solution for pure vapor condensation along a vertical plate. Since then several experimental and theoretical studies have been carried out for various geometries.

In the last decades, the effect of noncondensable gas on vapor condensation has been extensively studied. It has been found that the presence of a noncondensable gas leads to a substantial decrease in the condensation rate.

The aim of this work is to develop a numerical solution from the full set of governing equations for steam condensation in a vertical channel of parallel plates in the presence of a noncondensable gas. Parametric studies are carried out to examine the effect of different input parameters on the condensed flow rate. The model is applied to the vapor- air mixture.

In order to locate our work, we present in the first chapter a literature review of previous work on condensation. First, it presents the Nusselt theoretical model of pure vapor condensation on a vertical plate, then a summary of the main studies about pure vapor condensation and vapor-noncondensable gas mixtures.

The second chapter covers the description of the physical model (two vertical parallel plates), adopted simplifying assumptions and the mathematical formulation of the problem. We present the governing equations and the associated boundary conditions.

The third chapter is devoted to describe the solution method, the grid independence and the computer code validation.

In the fourth chapter, the obtained results and their interpretation are presented. We have studied the coupled heat and mass transfer with condensation in a vertical plate under asymmetric boundary conditions. In this study, the channel left wall is

kept isothermal and wet while the right one is adiabatic, dry and impermeable to matter. The study focus on a parametric study for water vapor condensation in presence of a noncondensable gas for forced convection. The set control parameters are the temperature, the relative humidity and Reynolds number at the channel inlet as well as the aspect ratio.

Finally, the present thesis ends up with the presentation of the main conclusions drawn from this work and the proposed perspectives.

Chapter I

LITERATURE REVIEW

I.1   Introduction

This chapter is devoted to a literature review about liquid film condensation phenomenon with steam convection on cold surfaces. First, we present some theoretical background about the different types of condensation, then an overview of some theoretical and experimental research conducted by different authors, considering mainly the following aspects: the studied geometry, the vapor state and flow regime.

The field of condensation owes its current state to the pioneering work of Nusselt [1] (1916).It involved a simplified model of laminar film condensation on a vertical isothermal flat plate. Since then, numerous researchers refined the solution by considering various conditions and different geometries using analytical, empirical or numerical approaches. Following his work, both external and internal flows with condensation have been studied extensively for various geometries and vapors.

I.2   Generalities

Condensation is a physical process of phase change of a pure substance from the vapor state to the liquid state. It occurs when the steam is in contact with a medium

whose temperature is lower than the steam saturation temperature and is accompanied by a significant heat release. Different types of condensation are marked according to the wettability of the surface and the various forms of the obtained condensate (Fig. I.1).

Filmwise condensation   Dropwise condensation

Figure I.1: Different types of condensation *(Heterogeneous condensation)*

I.2.1   Dropwise condensation

Dropwise condensation takes place if the condensate cannot wet the surface. The wettability can be measured by the contact angle with the surface. It states that liquid droplets form only heterogeneous at nucleate sites; if they are formed with a radius exceeding that of equilibrium, they will continue to grow and then join with surrounding droplets. Once the mass of the condensate reaches a critical point, it will be removed from the surface by gravitational forces or by drag forces produces by surrounding gas. As droplets are removed, the surface is wiped clean of condensate and the process restarts at the nucleate sites. This periodic cleaning constitutes the advantage of dropwise condensation over filmwise condensation, as there is no resistance to heat transfer through the condensate when the condensate layer is removed (the cooler wall surface always has an area that is not covered by condensate.); and thus the heat transfer increases significantly. Therefore, in industrial applications it is wise to introduce conditions that promote dropwise condensation.

I.2.2   Filmwise condensation

As in the case of external heterogeneous dropwise condensation, filmwise condensation occurs when a cold wall surface is in contact with a vapor near saturation conditions. Filmwise condensation on a vertical surface occurs when the liquid phase fully wets the surface, whereas in dropwise condensation the liquid incompletely wets the solid surface.

The condensation process begins with vapor condensing directly on the wall surface. However, in contrast with dropwise condensation, after the wall is initially wetted, it remains covered by a thin film of condensate. After that point, condensation occurs only at the liquid-vapor interface. Therefore, the condensation rate is directly a function of the rate at which heat is transported across the liquid film from the liquid-vapor interface to the wall.

The laminar regime was first rigorously analyzed by Nusselt [1](1916). Because many simplifying assumptions were made, this analysis provided a closed-form solution. This classical analysis was a very good building block for later studies that gradually chipped away at the assumptions made by Nusselt by employing numerical methods. The Nusselt analytical model will be presented in the next section, followed by some of the later studies that improved Nusselt's model. The improvements presented will include the consideration of noncondensable gases in the condensation process and the effect of vapor flow (Nusselt assumed a stagnant vapor reservoir). The wavy and turbulent regimes are obviously much more difficult to solve than the laminar, and numerical methods are required to obtain an acceptable solution. However, the overall heat transfer rate from the vapor reservoir to the cooled wall is dominated by contributions from the wavy and turbulent sections.

In many industrial applications the saturated vapor to be condensed is in fact a miscible binary vapor mixture. In a multi-component vapor, the saturation temperature is referred to as the *dew point*. This binary mixture condenses differently than a pure vapor and has lower heat transfer and condensation rates. A large resistance to heat transfer is produced in multicomponent system than in pure vapor, due to the buildup of the volatile component at the interface, because they have lower saturation temperature.

I.3   Nusselt analytical model

The classical analysis of laminar film condensation on a vertical or inclined wall was performed by Nusselt [1] (1916). As it is the case in any heat transfer analysis, the final goal is to obtain the heat transfer coefficient and the corresponding Nusselt number for the heat transfer device under consideration. Therefore, the objective of Nusselt analysis is to find the heat transfer coefficient and the Nusselt number for the laminar flow regime in film condensation on a vertical surface. The classical Nusselt analysis requires many assumptions in order to achieve a closed-form solution of the boundary layer type momentum equations. These assumptions include the following:

1.   The flow is laminar.

2.   Fluid properties are constant.

3. Subcooling of the liquid is negligible in the energy balance, i.e., all condensation occurs at the saturation temperature corresponding to the pressure in the liquid film near the wall.

4. Inertia and convection effects are negligible in the boundary layer momentum and energy equations, respectively.

5.   The vapor is assumed stagnant, and therefore, shear stress is considered to be negligible at the liquid-vapor interface.

6. The liquid-vapor interface is smooth, i.e., condensate film is laminar and not in the wavy or turbulent stages.

Since the vapor phase is stationary, the governing equations for the vapor phase are no longer needed. Only the continuity and the momentum equations for the liquid phase are needed, in which the pressure gradient may be approximated in terms of conditions outside the liquid film, as required by boundary layer approximation. It follows that pressure in the liquid film satisfies:

$$\frac{dp_l}{dx} = \frac{dp_v}{dx} = \rho_v g \tag{I.1}$$

The momentum equation is:

$$\rho_l \left(u\frac{\partial u}{\partial x} + v\frac{\partial u}{\partial y} \right) = \mu_l \frac{\partial^2 u}{\partial y^2} + g(\rho_l - \rho_v) \tag{I.2}$$

The left-hand side term represents the inertia effects in the slender film region, while the right-hand terms are the effects due to friction and the sinking effect. As stated by Assumption #4 of the above list, the inertia term is negligible in this analysis. Therefore, the above equation simplifies to

$$\frac{\partial^2 u}{\partial y^2} = \frac{g}{\mu_l}(\rho_v - \rho_l) \tag{I.3}$$

Integrating this equation twice with respect to y and using the boundary conditions of nonslip at the wall (u=0 at y=0) and zero shear at the liquid-vapor interface (du/dy = 0 at y = 5, Assumption #5) yields the following:

$$u(x, y) = \frac{(\rho_l - \rho_v)g}{\mu_l}\left(y\delta - \frac{y^2}{2}\right) \tag{I.4}$$

It can be seen from this equation that the downward velocity component is directly dependent on both the x and y coordinates due to the varying (increasingly thick in the x-direction) film thickness.

The mass flow rate per unit width of surface Γ, , of this liquid film at any point can be found by integrating the above velocity profile across the liquid film thickness and multiplying by the liquid density, i.e.,

$$\Gamma = \rho_l \int_0^\delta u\, dy$$

$$= \frac{\rho_l(\rho_l - \rho_v)g\delta^3}{3\mu_l} \tag{I.5}$$

Where it can now be seen that the mass flow rate is a function of the x-coordinate. Recalling that the heat transfer across the liquid film is by conduction only, and assuming that no subcooling exists at the liquid-vapor interface (Assumption #3), Fourier's Law can be used to obtain the heat flux across the film thickness:

$$q'' = \frac{k_l(T_{sat} - T_w)}{\delta} \tag{I.6}$$

Where T_{sat} and T_w are the saturation temperature and wall temperature, respectively.

The heat transfer rate per unit width for a control volume is given by:

$$dq' = \frac{k_l \Delta T}{\delta} dx \tag{I.7}$$

Where: $\Delta T = T_{sat} - T_w$

Since no subcooling in the liquid film exists, the latent heat effects of condensation dominate the process. Therefore, it can be said that:

$$dq' = h_{lv} d\Gamma \tag{I.8}$$

Where $d\Gamma$ is found by differentiating the expression for mass flow rate per unit surface. It is found to be:

$$d\Gamma = \frac{\rho_l(\rho_l - \rho_v)g\delta^2}{\mu_l} d\delta \tag{I.9}$$

This expression and the expression for heat flow dq' across the control volume are then substituted into the energy equation, and the following is found:

$$\delta^3 \frac{d\delta}{dx} = \frac{k_l \mu_l \Delta T}{\rho_l(\rho_l - \rho_v)g h_{lv}} \tag{I.10}$$

Finally, δ can be found by integrating the above and using the boundary condition that $\delta = 0$ at $x = 0$:

$$\delta = \left[\frac{4k_l \mu_l x \Delta T}{\rho_l(\rho_l - \rho_v)g h_{lv}} \right]^{1/4} \tag{I.11}$$

The local heat transfer coefficient hx, is found to be:

$$h_x = \frac{q''}{T_{sat} - T_w} = \frac{k_l}{\delta} = k_l^{3/4} \left[\frac{\rho_l(\rho_l - \rho_v)g h_{lv}}{4\mu_l x \Delta T} \right]^{1/4} \tag{I.12}$$

The local Nusselt number, Nu_x, of the laminar film condensation process on a vertical plate is found to be:

$$Nu_x = \frac{h_x x}{k_l} = \left[\frac{\rho_l(\rho_l - \rho_v)g h_{lv} x^3}{4k_l \mu_l x \Delta T} \right]^{1/4} \tag{I.13}$$

It is also desirable to obtain the average heat transfer coefficient and Nusselt number for a plate of length L. The mean heat transfer coefficient can be defined:

$$\bar{h} = \frac{1}{L} \int_0^L h_x(x) dx \tag{I.14}$$

The mean Nusselt number is :

$$\overline{Nu} = \frac{\bar{h}L}{k_l} = 0.943 \left[\frac{\rho_l(\rho_l - \rho_v)gh_{lv}L^3}{\mu_l k_l \Delta T}\right]^{1/4} \tag{I.15}$$

The local and average heat transfer coefficient can also be nondimensionalized in term of Reynolds number Re, defined as:

$$Re_\delta = \frac{4\Gamma}{\mu_l} \tag{I.16}$$

The Reynolds number for laminar film condensation is:

$$Re_\delta = \frac{4\rho_l(\rho_l - \rho_v)g\delta^3}{3\mu_l^2} \tag{I.17}$$

The following dimensionless correlations are obtained:

$$\frac{h_x}{k_l}\left[\frac{\mu_l^2}{\rho_l(\rho_l - \rho_v)g}\right]^{1/3} = 1.1 \, Re_\delta^{-1/3} \tag{I.18}$$

$$\frac{\bar{h}}{k_l}\left[\frac{\mu_l^2}{\rho_l(\rho_l - \rho_v)g}\right]^{1/3} = 1.47 \, Re_\delta^{-1/3} \tag{I.19}$$

Where the bracket term to the left of the equal sign, together with its exponent (1/3), is the characteristic length.

The above Nusselt analysis assumes no subcooling in the liquid condensate. This assumption can be removed by making an energy balance at the interface that takes subcooling of the liquid into account, as follows:

$$\frac{dq'}{dx} = \frac{k_l\Delta T}{\delta} = h_{lv}\frac{d\Gamma}{dx} + \frac{d}{dx}\int_0^\delta \rho_l c_{pl} u(T_{sat} - T)dy \tag{I.20}$$

The final term of the right-hand side takes into account a temperature gradient across the liquid condensate film. Using a linear temperature profile,

$$\frac{T_{sat} - T}{T_{sat} - T_w} = 1 - \frac{y}{\delta} \tag{I.21}$$

The energy balance can be written as:

$$\frac{k_l\Delta T_l}{\delta} = h_{lv}'\frac{d\Gamma}{dx} \tag{I.22}$$

where

$$h_{lv}{}' = h_{lv} \left\{ 1 + \frac{3}{8} \left[\frac{c_{pl}(T_{sat} - T_w)}{h_{lv}} \right] \right\}$$

(I. 23)

I.4   Pure vapor condensation

Nusselt assumptions considerably restrict the practical application of these equations. In fact, the actual conditions of condensation are generally very different from those of Nusselt model: high vapor velocity or turbulent flow, variable pressure, significant effects of the shear stress at the liquid-vapor interface, laminar flow of liquid film with waves or turbulent, nonuniform wall temperature, physical properties of fluids varying with temperature,... A lot of work has been done by various authors to make improvements to the Nusselt model by integrating neglected terms in this model and evaluate their influence on the evolution of condensation and heat transfer coefficients.

The first correction to Nusselt model was done by Rohsenow [2] who improved this analysis even more by including the effects of convection in the liquid along with liquid subcooling, and thereby developing the following:

$$h_{lv}{}' = h_{lv} \left\{ 1 + 0.68 \left[\frac{c_{pl}(T_{sat} - T_w)}{h_{lv}} \right] \right\}$$

(I. 24)

Where $Ja = \frac{c_{pl}(T_{sat} - T_w)}{h_{lv}}$ which represents the ratio of sensible heat to latent heat.

So, the result is that the convection effects in the liquid are as much high as Ja number is high. Otherwise, Rohsenow solution leads to a lower liquid film thickness than that obtained by Nusselt model.

Sparrow and Gregg [3] have used the boundary layer equations to study the condensation of stagnant saturated vapor on a vertical plate with taking the inertia terms and enthalpy convection into consideration. The pressure gradient and shear stress at the interface were neglected. The physical properties of fluids were assumed to be constant. Using affine transformation method and introducing the stream function, the partial derivative equations were transformed to ordinary differential equations then solved numerically. They have shown that for high values of Prandtl

11

number of liquid Pr_L, the effects of convection term of enthalpy cannot be neglected. Whereas, for low values of Jacob, they have established the following relation (a bit different from that of Nusselt) for calculating the mean HTC during stagnant vapor condensation on a horizontal cylinder of diameter D:

$$\bar{h} = 0.733 \left(\frac{L_c g \rho_L^2 \lambda_L^3}{\mu_L (T_s - T_w) D} \right)^{1/4} \tag{I.25}$$

Koh et al. [4] introduced some modifications into Sparrow and Gregg model concerning water vapor condensation on a vertical isothermal wall, taking into account shear stresses at the liquid-vapor interface. The vapor is driven by the flow of the liquid film. Transfers in both liquid and vapor phases are described by boundary layer equations. The coupling of equations at the interface is provided by the continuity of velocities and shear stresses. Using affine transformation method allows to convert the partial derivative equations to ordinary differential equations system then solved numerically. They highlighted the intervention of the parameter $R = (\rho_L \mu_L / \rho_v \mu_v)^{0.5}$ resulting from the equality of shear stresses at the interface. The results show that for liquids with high Prandtl number (of ten or greater), the effect of interfacial stresses is negligible. For liquids with low Pr_L, taking into account the shear stresses at the interface leads to a reduction of the heat flux density.

Koh [5] has developed a flowing vapor condensation model with forced convection along a horizontal flat plate. He reused the affine transformation method for solving equations, after removing gravity term. The results show that the liquid velocity profile is roughly linear for low film thickness. For low Pr_L numbers, the temperature profile is linear and the effect of liquid enthalpy convection term is negligible. However, For liquids of high Prandtl number (Pr > 1), solutions indeed depend on the Prandtl number, where the energy transfer by convection cannot be neglected.

Shekriladze and Gomelauri [6] have studied vapor condensation in laminar flow with forced convection along a horizontal plate. They assumed that the shear stress at the liquid-vapor interface equals to the loss momentum quantity of condensed vapor. This assumption simplifies the problem by decoupling the equations of both vapor and liquid phases. Furthermore, neglecting terms of inertia, convection and pressure gradient, simple solutions have been developed. The authors also have confirmed that

the influence of enthalpy convection terms of the liquid is negligible for low Prandtl numbers.

Dobran and Thorsen [7] conducted a theoretical study of laminar film condensation in forced flow of pure saturated vapor in a vertical tube with isothermal wall. The vapor velocity profile at the inlet is assumed to be negligible. The model is developed with taking into account the terms of axial pressure gradient, inertia, shear stresses at the interface in the motion equations of both phases and enthalpy convection terms in liquid film energy equation. In their analysis, it was found that the condensation process is governed by five parameters, which are the ratio of vapor Froude to Reynolds number, Buoyancy number, vapor to liquid viscosity ratio, liquid Prandtl number and Subcooling number. The analysis has led to determine the physical parameters characteristic of the problem. For the resolution of transport equations, the authors introduce a simplifying assumption of profiles of vapor velocity, liquid velocity and liquid temperature. Comparison of the results with Nusselt's analytic solution of constant interphase shear is also made and it was found that at high pressures, high Prandtl numbers and high ratios of Froude to Reynolds numbers, his analytic solution underpredicts the condensation length and film thickness and overpredicts the interphase mass and heat transfer. Significant disparities at low Prandtl numbers were found between analytic and numerical solutions for heat-transfer results as well as the hydrodynamic results. These disparities are a consequence of neglecting inertia terms in the liquid and vapor equations of motion in the analytic model and their inclusion in the model presented in this work.

Shang et al. [8] proceeded to theoretical study about laminar film condensation of a pure saturated vapor on an isothermal vertical plate at atmospheric pressure with consideration of the various factors including the variable thermophysical properties. Laminar boundary layer equations are applied in the two phases. A temperature parameter method and a polynomial approach were used to treat variable thermophysical properties for both vapor and liquid films. The dimensionless velocity component method was used to transform the system of partial differential equations associated with the two-phase boundary problem into a system of dimensionless ordinary equations. According to the numerical solutions and with a curving matching method, the corresponding simple and practical correlations of heat transfer coefficient and mass flow rate were developed by means of the superheated

temperature of vapor and the subcooled temperature of a plate besides the defined local Grashof number of liquid film.

They have concluded that the subcooled temperature on the wall, and the superheated temperature of steam, dominate the dimensionless temperature gradient as well as the mass flow rate parameter, which demonstrate that the subcooling and superheating affect the heat transfer coefficient and mass flow rate for the film condensation of superheated steam.

Oh and Revankar [9] conducted a theoretical study for complete condensation for the vertical tube passive condenser. The modified Nusselt film model with a correction factor and the Blangetti model were compared with the experimental data. For the interfacial shear, the effect of mass transfer at the interface derived from Couette flow analysis was considered. For small film Reynolds number and small interfacial shear conditions, predictions from the modified Nusselt model agree well with the data. The condensation rate increases and the condensation heat transfer coefficient decreases as the system pressure increases. The overall trends of the analysis results are consistent with the classical Nusselt analysis for the pure steam condensation such as the local condensation heat transfer coefficient varies with the axial distance at the rate, the average condensation heat transfer coefficient varies with the tube length and temperature difference between vapor and film.

Finally, if it is desirable to include the effects of vapor superheat in the above analysis, the obtained latent heat can be further modified by adding $c_{pv}(T_v - T_{sat})$. The above analysis can also be applied for condensation outside a vertical tube if δ/D<<1,where D is the diameter of the tube. For an inclined wall with an inclination angle of θ(the angle between the wall and the vertical direction), the component of the gravitational acceleration along the inclined wall is g cosθ.

I.5   Condensation of vapor in presence of noncondensable

In most industrial processes where condensation occurs, the presence of noncondensable gases is unavoidable. The experimental results have shown the significant influence of noncondensable gases on condensation process. Indeed, even if they are present in small amount within the steam, they contribute to significantly reduce the condensation rate and the heat transfer between the gas mixture and the cold wall. Indeed, according to Dalton's law, the total pressure of a gas mixture is the sum of the partial pressures of its components. The partial vapor pressure decreases at the interface because of the vapor condensation resulting in a decrease of the vapor saturation temperature at which condensation occurs. On the other hand, the partial pressure of gas increases, which leads to an accumulation of gas at the interface, forming a concentration gradient and a thermal resistance to steam condensation in the interface vicinity. It results in a reduction of the heat transfer coefficient by condensation. The theoretical modeling of this problem is more complex than pure vapor condensation, due to the addition of the gas diffusion and the simultaneous presence of several transfer phenomena with a two-phase flow.

For this purpose, a two-dimensional theoretical model analysis of laminar film condensation of steam - air mixture on a vertical plate was developed by Minkowycz and Sparrow [10]. They conducted a theoretical study by considering the superheated mixture flowing or stagnant with varying physical properties. Wide ranging analytical investigation of laminar film condensation was presented. The studied situation is an isothermal vertical plate with steam as the condensing vapor and air as the noncondensable gas. In addition to the noncondensable gas, the analytical model includes interfacial resistance, superheating, free convection due to both temperature and concentration gradients, mass diffusion and thermal diffusion, and variable properties in both the liquid and the gas-vapor regions. Heat-transfer results are obtained for a wide range of parameters including bulk concentration of the noncondensable gas, system pressure level, wall-to-bulk temperature difference, and degree of superheating. It is demonstrated that small bulk concentrations of the noncondensable gas can have a decisive effect on the heat-transfer rate.

For instance, for a bulk mass fraction of air equal to 0.5 per cent, reductions in heat transfer of 50 per cent or more are sustained. The influence of the noncondensable gas is accentuated at lower pressure levels (Low saturation temperatures). It is shown that

the superheating has an opposite effect of noncondensable gas, and the heat transfer increase with the degree of superheating.

They demonstrated that when the noncondensable gas and/or superheating are involved, then the presence of the interfacial resistance precludes an exact solution and local similarity must be employed.

For pure vapor, it is demonstrated that heat transfer is almost independent to bulk saturation temperature at a given degree of superheating and independent of thermal driving force, and the free convection is insignificant.

It is shown that the aforementioned reductions in heat transfer are due entirely to the diffusional resistance of the gas-vapor boundary layer. The interfacial resistance is shown to be a second order effect. A similar finding applies to thermal diffusion and diffusion thermo. The effect of superheating, which is very small in the case of a pure vapor, becomes much more significant in the presence of a noncondensable gas. A reference temperature rule is deduced for extending the Nusselt model to variable-property conditions.

Wang and Tu [11] have developed a model to analyze the effect of noncondensable on film condensation of vapor-gas mixture in turbulent forced flow through vertical tube. It was found that the effect of noncondensable gas on condensation is more significant in ducts than in an unconfined space, because in the former case the mass fraction of inert gas in the free stream becomes more and more as condensation proceeds along the condensing surface. The effects are more strongly manifested in the vertical orientation of the tube than in the horizontal one. The heat transfer decreases monotonically as the mass fraction of the noncondensable gas increases (Fig.I.2 & .I.3). The reductions in heat transfer due to the noncondensable gas are accentuated at low operating pressures. As the inlet velocity of the mixture decreases, the effects become more and more appreciable (Fig.I.3).

Heat and mass transfer study for a natural convection between two vertical parallel plates with a water film or ethanol has been done by Yan and Lin [12]. Their results show the hypothesis of thin film is valid for small mass flow rate.
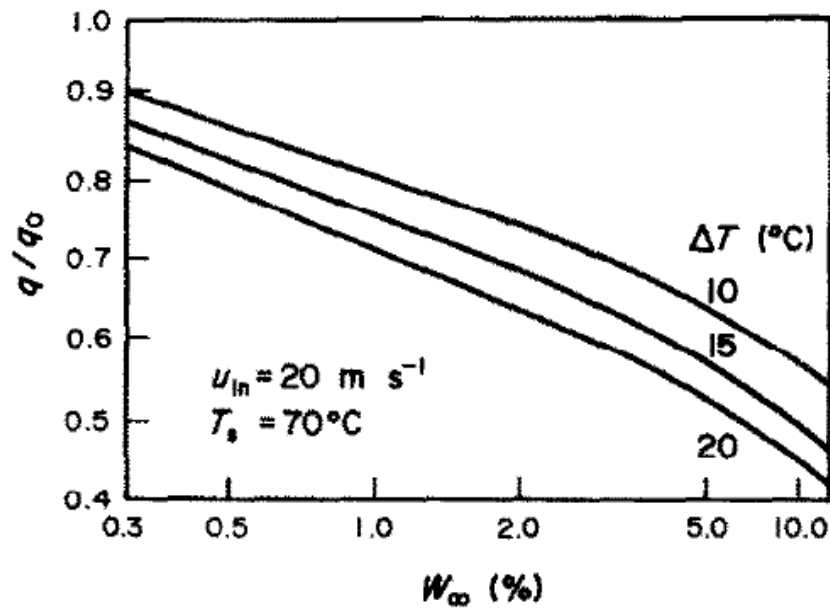
Figure I.2: Effects of noncondensable gas on condensation heat transfer in the vertical tube under sub-atmospheric pressure.
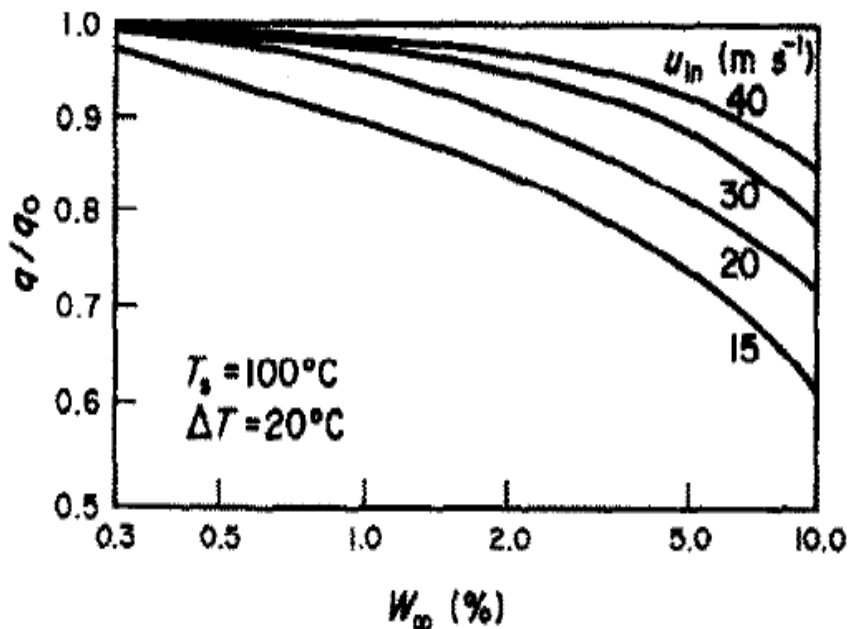
Figure I.3 : Effects of noncondensable gas on condensation heat flux for different inlet velocities.

Munoz-Cobo et al. [13] have developed a model for annular filmwise condensation inside vertical tubes when noncondensable gases are present. The local heat transfer coefficient was calculated and the results were compared with experimental data. It was seen that in the turbulent region and at high Reynolds number the heat transfer coefficients strongly depend on the interfacial shear stresses which in turn depend on the correlation used to calculate the interfacial friction factors, where, near the tube inlet the heat transfer coefficients change sharply with distance(Fig.I.4). This sudden change is due mainly to the fact that interfacial shear stress effects on the condensate

17

film thickness are very important near the tube inlet. The model developed in this paper provides good results in the turbulent region and with moderate mass fractions of noncondensable gases. Ranging from 1 to 10%. The developed model accounts for: (i) shear stresses produced by concurrent downflow, (ii) condensation effects on sensible heat transfer and interfacial shear stresses, (iii) noncondensable gas effect on the heat transfer coefficients. Moreover, the influence of the condensation process on the Sherwood number has been taken into account.
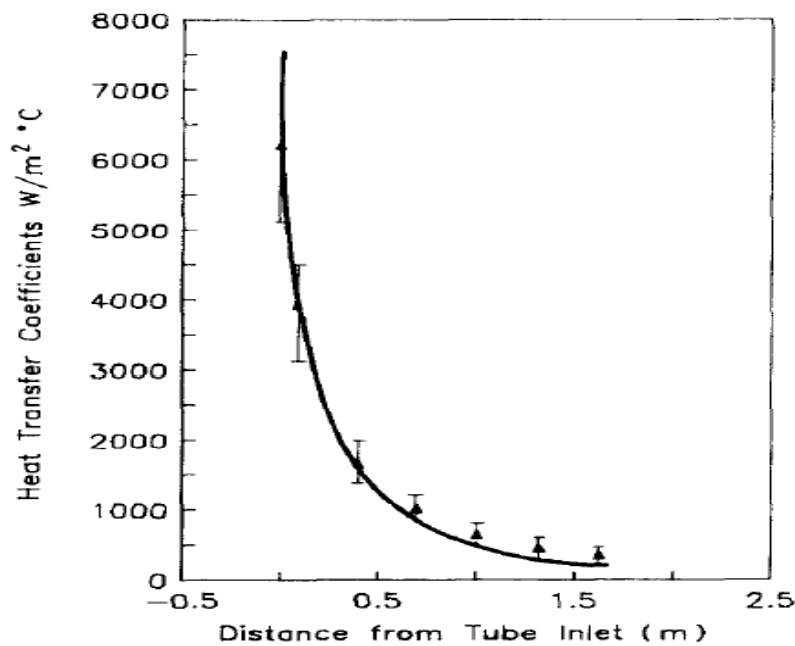
Figure I.4: Variation of heat transfer coefficients along the length of the condenser. Experimental points from Siddique et al. The continuous line shows the theoretical prediction

A theoretical model has been developed by Maheshwari et al. [14] to study the local heat transfer coefficient of a vapor in the presence of a noncondensable gas, where the gas/vapor mixture is flowing downward inside a vertical tube. The gas/vapor core has been modeled using the analogy between heat and mass transfer. The liquid film flow is governed by modified Nusselt model to take into account film waviness effect on gas/vapor boundary layer. Results showed that the thermal resistance offered by gas/vapor boundary layer due to the condensation is higher than that offered by condensing film for low inlet Reynolds number. But this phenomenon may get reversed

at higher Reynolds number. As the inlet mixture Reynolds number increases, the condensation heat transfer coefficient increases due to the higher turbulence in the gas/vapor boundary layer.

Ait Hammou et al. [15] have conducted to a numerical study on downward laminar flow of humid air in an isothermal vertical channel with wet walls for mixed convection. The entering air is always warmer than the channel walls but its absolute humidity can be higher or lower than the one corresponding to the wall temperature. Thus, cooling of the air stream is accompanied by either condensation or evaporation, where, Condensation occurs when the vapor mass fraction at the inlet is higher than the corresponding saturation value at the wall temperature. In the opposite case, evaporation takes place. The transfers in air are described by the equations of conservation of mass, momentum, conservation of energy and species conservation, with taking into account the axial diffusion terms. The equations are elliptical; they are solved by finite volume method. The results show that for fixed wall conditions an increase of the inlet air temperature results in a small increase of the sensible Nusselt number and a significant decrease of the latent Nusselt number (fig .I.5 et I.6). The effect of buoyancy forces on the latent Nusselt numbers is small. On the other hand, the axial velocity profiles, the friction factor, the sensible Nusselt number and the Sherwood number are significantly influenced by buoyancy forces. The friction factor and the Sherwood number increase with both inlet air temperature and inlet air humidity.
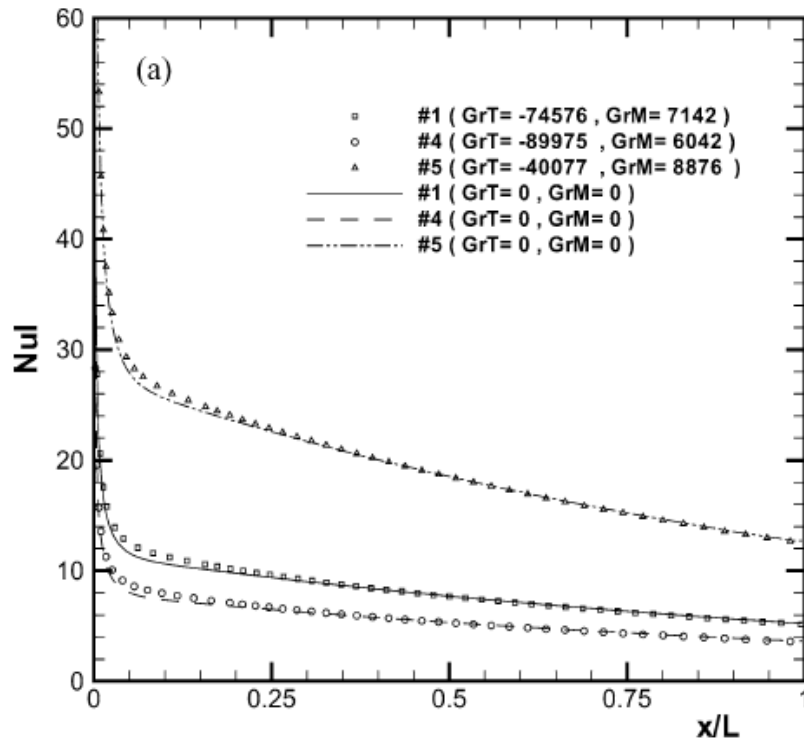
Figure I.5: Axial evolution of the latent Nusselt number.
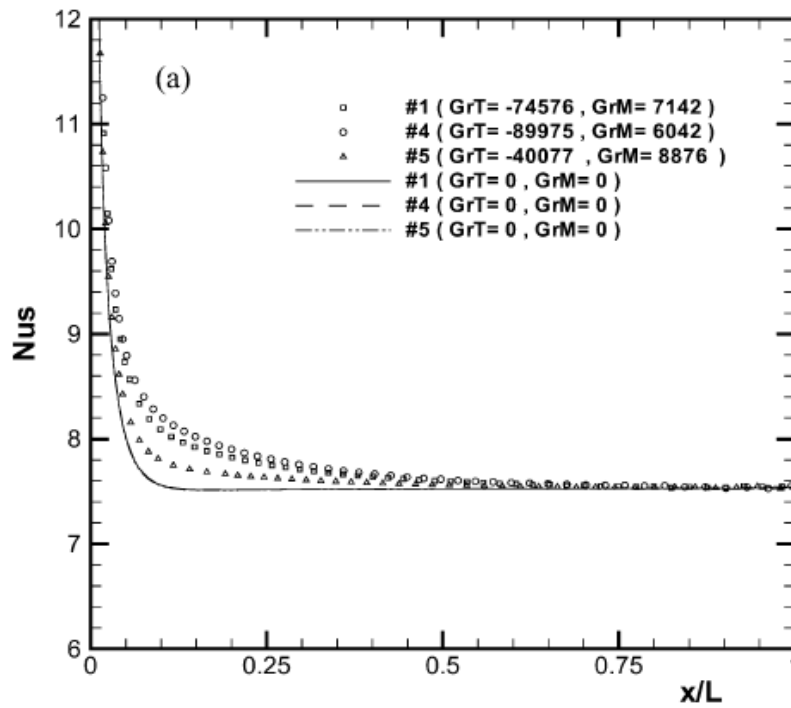

Figure I.6: Axial evolution of the sensible Nusselt number.

Oh et al. [16] have presented an experimental and theoretical study for a vertical tube condensation system with the presence of the noncondensable gas. Condensation experiments were performed with a vertical tube condenser, which is submerged in the secondary water pool where the condensation heat transferred from the tube is removed by the boiling. The results show that the condensation heat transfer rate and the condensation HTC decreases as inlet NC gas mass fraction increases , and higher steam flow results in higher condensation HTC. Otherwise, a heat and mass analogy model is developed to predict the filmwise condensation with the noncondensable gas. This model uses the momentum, heat and mass transport correlations selected from the general relationships, with taking into account the effects of the surface suction at the condensation interface. The liquid film thickness is determined from a mass balance in the condensate. The analysis results of the model were compared with experimental data and the agreement was satisfactory. For a large film Reynolds number region, the model slightly underestimates the condensation heat transfer coefficient due to the heat transfer enhancement by the film waviness. The enhancement of heat transfer is due to the waviness effect, which was not taken into account in this model.

Groff et al. [17] conducted a numerical analysis for film condensation from a turbulent gas–vapor mixture in axisymmetric downward flow in a vertical tube, based on the complete two-phase parabolic governing equations. A finite volume method was used for discretization of the governing equations of conservation of mass, momentum and energy in each of the liquid film and the mixture regions. A marching, fully coupled solution scheme is used on a mesh that adapts to the changing film thickness, which is a solution variable. Three turbulence models were used in each of the two phases. The axial velocity, transverse-direction mass flux, temperature, gas mass fraction, film thickness, and local axial pressure gradient were computed using a fully coupled approach, with the turbulence model equations solved separately. A comparative analysis for a wide range of operating conditions show that the k-ɛ turbulence model for both phases leads to the best agreement with the experimental data compared to other models. In addition, a parametric study was performed on the effect of changing the inlet Reynolds number, the inlet-to-wall temperature difference, and the inlet gas mass fraction for steam-air mixtures. An increase in the inlet Reynolds number produced a film that is thinner near the inlet due to significant interfacial shear effects, but thicker overall further down the tube. An increase in the inlet-to-wall temperature

difference produced thicker films due to a higher rate of condensation. Finally, an increase in the inlet gas mass fraction produced a thinner film due to the build-up of gas at the liquid-mixture interface and a resultant reduction in the rate of condensation.

Dharma Rao et al. [18] have developed a theoretical model for the case of in-tube laminar film condensation of water vapor in the presence of high concentration noncondensable gas, when the gas–vapor mixture flows inside a vertical tube under laminar forced flow conditions. The model is developed by considering the classical boundary layer equations with neglecting the convective term in the equations of the liquid phase. Liquid-gas interface temperature and condensate film thickness are calculated by considering the heat balance and mass balance at the interface. The equations have been solved numerically using finite difference method. Numerical results were obtained for wide range of the system parameters at inlet, such as relative humidity, temperature of vapor–gas mixture, gas phase Reynolds number and total pressure. From the numerical results the local and average Nusselt numbers, condensate Reynolds number, gas–liquid interface temperature and pressure drop were estimated. The variation of local gas–vapor mixture temperature along the length of the pipe was also estimated. It has been shown that the condensation heat transfer coefficients and the rate of condensation decreases considerably in the presence of noncondensable gas in high percentage. The authors have demonstrated that liquid Nusselt and Reynolds numbers increase with the inlet temperature, relative humidity and gas phase Reynolds number, but, they decrease when the inlet total pressure increases. However, the effects of these parameters on the gas phase Nusselt number are less important.

A mathematical model has been developed by J.D. Li et al. [19] to study the condensation of water vapor in the presence of noncondensable gas in condensers. The model includes the heat and mass transfer in the mixture channel, the heat transfer in the condensate film, condenser wall and the coolant channel. A numerical scheme was presented to solve the differential and algebraic equations. The model has been used to predict the condensation rate, the bulk temperatures of the coolant and the gas–vapor mixture, and the surface temperatures of the condenser wall. The predicted results for counter flow tube condensers were compared with three sets of published experimental data for system in which air is the noncondensable gas. It was found that

the predicted condensation rates and the bulk temperatures of the coolant agree very well with the experimental results. The model predictions and all the experimental results presented showed that the wall temperature of the condenser can be much higher than the bulk temperature of the coolant which showed that it would be very difficult to select a constant wall temperature (or constant heat flux) in modeling condensation from heat and mass transfer in the mixture channel alone. Because of the large temperature difference between the condenser wall and the coolant, it was found that the buoyancy effect on heat transfer in the coolant channel is in general large and cannot be neglected.

Kassim et al [20] conducted a numerical study to investigate the effect of the inlet air humidity in an upward airflow for a vertical channel. The zero film thickness model has been used. It has been found that the increase of inlet humidity affects seriously the performance of the humidifier as it induces condensation of the water vapor on the walls.

Li [21] has studied the condensation of water vapor in the presence of noncondensable gas in a vertical cylindrical tube using CFD simulation. Both heat and mass transfer in the gas mixture and the heat transfer in the coolant flowing in the annulus channel has been included. Because of this, no assumptions have been made of the wall temperature, heat flux or heat transfer coefficient at the condenser tube wall which could be predicted from the CFD simulation. The CFD simulations of the flow inside the tube condenser of gas mixture were carried out on the gas mixture only. The effect of the condensate film on the gas mixture flow was accounted for through a set of new boundary conditions including the sources for the mass, momentum and energy, a slip boundary condition for the axial velocity and a revised wall temperature taking into account the film thickness. The condensate film thickness was estimated using the Nusselt method by assuming that the shear stresses of both the gas mixture and the condensate match each other at the interface between the gas mixture and the condensate film. The axial velocity of the gas mixture was assumed to match that of the condensate at the interface. The CFD simulation results have been compared with the experimental results. It was found that the CFD simulation results in general agree well with the measured quantities such as the adiabatic wall temperature, the centerline temperature of the gas mixture and the wall temperature of the condenser tube wall.

The simulation results showed that for the condensation of high mass fraction of water vapor in the presence of noncondensable gas, the heat transfer in the coolant channel was the limiting factor. The results showed that the average axial velocity decreases rapidly as water vapor is condensed, the density of the gas mixture increases across the condenser tube and along the condenser and the axial velocity of the gas mixture at the interface between the gas mixture and the condensate film is not small. For lower Reynolds numbers of gas mixture at the inlet or long enough condenser tube with high mass flow rate of coolant, the axial velocity of the gas mixture at the interface can be higher than the average axial velocity of the gas mixture.

C. Chantana and S. Kumar [22] have conducted a theoretical model using heat and mass analogy to study heat and mass transfer characteristics of water vapor condensation in the presence of air as a noncondensable in a vertical annulus tube for low inlet water vapor mass fraction. The condenser tube surface temperature is below the vapor dew point temperature due to coolant flow in the inner tube. The interface temperature is determined iteratively along the condenser length. The roughness and suction effects have been incorporated into the model because they have an influence on heat and mass transfer rate (they enhance it). The latter is due to the steep gradient of temperature and concentration near the interface. The predicted condensation rates were computed by summation the vapor condensation rate of all the elements divided along the tube length. It was shown that the condensation rate increases with increasing Reynolds number and inlet water vapor fraction (by increasing interface temperature). It has been seen that Nusselt and Sherwood numbers without including the effects are less than those which including these enhanced effects. It has been shown that the sensible heat transfer coefficient could not be neglected at low water vapor inlet fraction (the same case for low Re). However, at higher water vapor fraction (the same case for high Re), the sensible heat transfer coefficient can be omitted and the effect of condensation heat transfer coefficient to the overall heat transfer coefficient is more pronounced. It has been found that the increase of the inlet vapor mass fraction and the Reynolds number leads to an increase of the interface temperature.

Recently, F. Hassaninejadfarahani et al. [23] have presented a numerical solution for laminar film condensation in a vertical tube. The model is based on the complete parabolic governing equations. The flow conditions with very high inlet gas mass

fractions (more than 0.8) have been predicted through the fully coupled marching solution method. The input data are inlet Reynolds number, inlet pressure, inlet temperature, inlet relative humidity, tube radius, tube length, and wall temperature. New results including axial variation of bulk air mass fraction, bulk temperature, interface air mass fraction, interface temperature, local Nusselt number, film thickness, and proportion of latent heat transfer have been presented. A comparison has been made between results from this study and previous ones shows that they have similar trends. It has been found that the velocity in the mixture attains a more parabolic profile as the distance from the inlet increases. Also, the temperature profile has a parabolic shape for the gas mixture, but it has nearly linear profile in the liquid region. It has been observed that interface temperature increases along the length of the tube. It has been shown that near the inlet, air mass fraction is equal to that of the inlet for most of the cross section and increases rapidly near the interface due to the interface impermeability condition. It has been found that the condensate film thickness increases with increasing inlet Reynolds number (after some distance from the inlet), increasing relative humidity, and increasing inlet-to-wall temperature difference. They have shown that an increase of tube radius for a fixed Reynolds number lead to a decrease of the condensation rate and the film thickness, where they increase with increasing inlet temperature.

More recently, Giri et al [24] made a computational study on mixed convection for a vertical channel under simultaneous heat and mass transfer representing condensation on parallel plates. Local variation of sensible heat Nusselt number and condensation Nusselt number are presented and induced velocity, pressure drop, overall sensible heat Nusselt number, overall condensing Nusselt number were correlated with different governing parameters (Pin, Gr_t, Gr_m, Re, Ja and L). It is found that both the local sensible heat Nusselt number and local condensing Nusselt number decrease monotonically along the axial direction and each of the quantities reaches a fully developed value far downstream. Fully-developed local sensible Nusselt number neither depends on inlet velocity nor inlet pressure. However, fully developed condensing Nusselt number does depend on velocity and inlet pressure, where the rise of velocity and the reduction of inlet pressure lead to an increase in the condensing Nusselt number.

I.6   Conclusion

From this review, it was found that for theoretical analyses of vapor condensation in the presence of a noncondensable gas, one of two techniques is usually employed: boundary layer analysis or heat and mass transfer analogy. For the boundary layer analysis, the governing conservation equations are solved. These equations are solved using an integral approach, assuming similarity, or via another numerical method. The heat and mass transfer analogy is based on a heat balance at the liquid-mixture interface where the heat transferred from the mixture is equated to the heat transferred through the condensate film. The heat transfer from the mixture phase is made up of sensible heat and the latent heat given off when the vapor condenses.

In this work, we consider the vapor condensation as a liquid film in presence of a noncondensable gas for forced convection in vertical channel of parallel plates. This geometric configuration is particularly interesting which is a good approximation for a rectangular duct because it is commonly used in industrial installation (compact heat exchangers, condensers...). Furthermore, this channel analysis can be readily extended to the case of a vertical pipe, which has many important industrial applications.

The liquid film is assumed to be thin. This hypothesis, known in the literature as the *zero film thickness model*, allows us to handle only the conservation equations in the gas flow with the appropriate boundary conditions. The liquid film temperature is supposed to be the imposed wall temperature.

For this purpose, it is proposed to develop a numerical model for forced convection about the being considered physical model (see fig.II.1). The study is carried with taking into account some parameters often neglected in condensation studies, namely the axial pressure gradient, axial diffusion.

The objective is to perform a full analysis of the phenomenon of condensation for determining changes in temperature, mass fraction of steam in the gas mixture, the condensed mass flow rate, sensible and Latent Nusselt number. The effect of important parameters characteristic of condensation on the evolution of these parameters will also be considered, in particular the inlet temperature, relative humidity, Reynolds

number and the distance between walls for vertical channel. The applications selected for analysis concern water vapor-air mixtures.

Chapter II

MODEL DESCRIPTION

II.1   Introduction

The study being considered presents film condensation for forced convection of water vapor in presence of noncondensable gas through a vertical channel and in space limited between two vertical plates.

This chapter presents a description of the physical model, adopted simplifying assumptions and mathematical model will be used in this work. Liquid water film flows on the internal face of the isothermal plate, which is maintained at a uniform temperature T_w.The liquid film is assumed to be extremely thin. This hypothesis, known in the literature as the *zero film thickness model*, allows us to handle only the conservation equations in the gas flow with the appropriate boundary conditions.

II.2   Problem Statement

The diagram of the problem under consideration is shown in Figure II.1. A mixture of a saturated vapor and a noncondensable gas enters a vertical channel of 2H width, with a:

- ✓ uniform temperature profile, T_{in};
- ✓ uniform velocity profile, u_{in};and
- ✓ uniform gas mass fraction, W_{in}.

The temperature of the left wall is maintained lower than that of the inlet mixture resulting in vapor condensation and a liquid film developing along the length of the channel, where the right wall is adiabatic and nonpermeable. The mixture entering the channel is laminar for cases of low inlet Reynolds numbers. The channel is crossed by a downward flow of humid air for a steady state case. The studied physical model allows the problem to be modeled as two-dimensional.
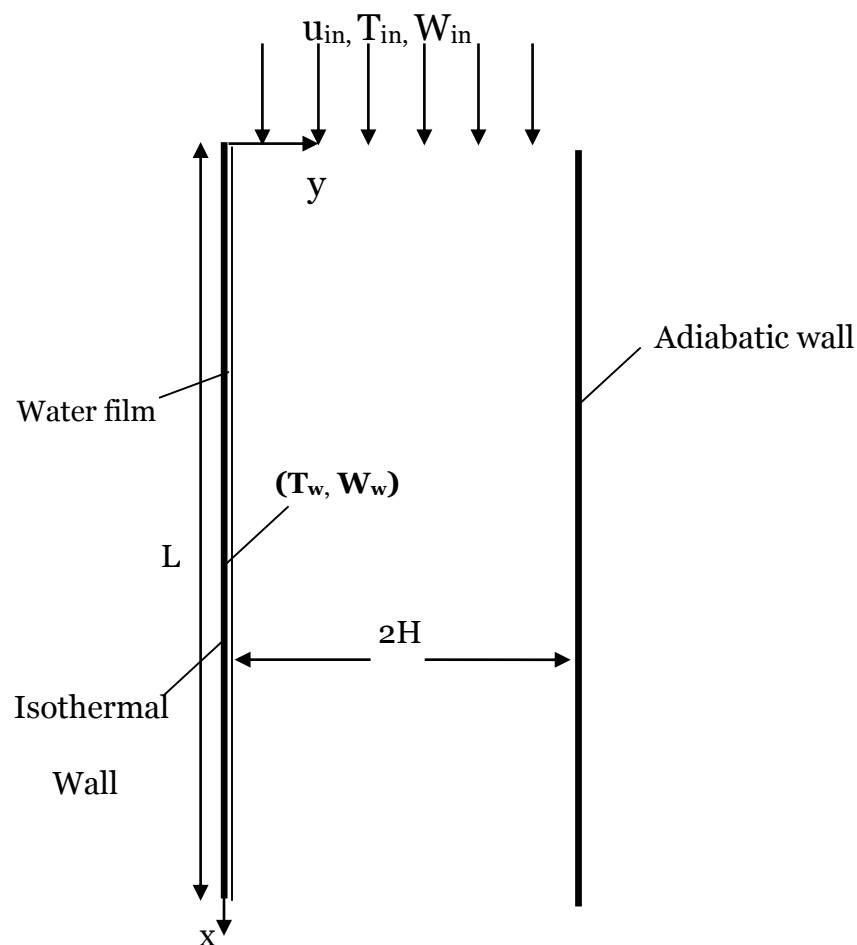

Figure II.1: Physical Model

II.3   Assumptions

The following assumptions were made when formulating the governing equations:

Each assumption will be followed by the reason for assuming it.

✓ The flow is steady state ;

- All the properties and flow conditions are assumed to be independent of time and therefore, variation with respect to time will not be considered.

✓ The mixture is Newtonian fluid;

- Most fluids allow writing that the shear stresses in both phases are proportional to transverse velocity gradient (or strain rate).

✓ The flow is laminar, Incompressible, two-dimensional;

- The fluid flow regime is based on Reynolds number criteria for gas mixture(Re). So, assuming that gas mixture flow in channel remains laminar for the range used in our study. The density does not vary as function of the pressure. This hypothesis has been used by many researchers, even for Reynolds number that exceed 1000. We name for example: Lin et al. [25], Debbissi et al. [26] and Siow et al. [27].

✓ The vapor-gas mixture is treated as an ideal gas mixture – The mixture is treated as a binary mixture of two ideal gases. The density is determined from the ideal gas law and the total pressure is the sum of the partial pressures of the gases;

- The gas mixture phase can be similar to a mixture of two ideal gases for relatively low pressures (Do not exceed some atmospheres). EOS for ideal gases can be used.

$$P_k = {\rho_k RT}/{M_k} \quad \text{where: } [k = g, v] \tag{II. 1}$$

$$P = P_g + P_v \tag{II. 2}$$

✓ Saturation conditions are assumed at the liquid-mixture interface;

- At the liquid –mixture interface where condensation occurs, the vapor must be saturated; therefore, the interface temperature will equal the saturation temperature corresponding to the vapor partial pressure.

✓ Viscous dissipation is neglected;

- The viscous dissipation is insignificant due to low-speed in the under consideration study (Debbissi et al. [26]).

- ✓ Constant thermophysical properties according to *one-third rule*.
    - They are evaluated at reference temperature and reference mass fraction. This way of evaluating thermo-physical properties has been used by many authors, where reference temperature T_{ref} and mass fraction W_{ref} obtained by these expressions: $T_{ref} = (2.T_w + T_{in})/3$ and $W_{ref} = (2.W_w + W_{in})/3$, where T_w, T_{in}, W_w and W_{in} are respectively the channel wall and inlet air temperatures and mass fractions. This way of evaluating thermo-physical properties, known as the one-third rule, has been used previously in the literature (Hubbard el al. [28]; Chow & Chung [29]).

- ✓ Soret and Dufour effects are neglected.
    - The mass flux caused by the temperature gradient (Soret effect) and the heat flux caused by the concentration gradient are negligible. These secondary effects are not taken because the temperature and concentration are small (Aguanoun et al. [30]).
- ✓ The transfer by radiation is negligible.
    - Since the considered temperature interval stay low, the effect of radiation of the walls can be neglected.
- ✓ The liquid film is thin;
    - To treat the liquid film as a boundary condition, the film is considered thin. So its temperature equals to that imposed on the wall. This allows us to solve the conservation equations only in the gas phase. This hypothesis has been widely used in the literature (Gebhart and Pera, [31], Lin et al. [25], and Kassim [32]). This hypothesis, known in the literature as the *zero film thickness model*, allows us to handle only the conservation equations in the gas flow with the appropriate boundary conditions. The liquid film is supposed to be at the imposed wall temperature. The validity of this assumption has been investigated by Yan [33] for both air-water and air-ethanol systems.

II.4   Mathematical model

The mixture was defined by a set of governing equations in the x-y coordinate system.

x: the axial coordinate measured in the flow direction.

y: the normal coordinate to x.

The transport phenomena in the gas mixture are described by the continuity, momentum, energy and mass-diffusion equations following the classical boundary layer model.

II.4.1   Equations govern the Hydrodynamic, thermal and mass fields

By adopting the simplifying hypotheses indicated in the previous paragraph, the equations that govern the heat and mass transfer in a vertical channel can be written as follows:

Continuity Equation

$$\frac{\partial u}{\partial x} + \frac{\partial v}{\partial y} = 0 \tag{II.3}$$

Momentum Equation following x

$$\rho\left(u\frac{\partial u}{\partial x} + v\frac{\partial u}{\partial y}\right) = -\frac{\partial p}{\partial x} + \mu\left(\frac{\partial^2 u}{\partial x^2} + \frac{\partial^2 u}{\partial y^2}\right) \tag{II.4}$$

Momentum Equation following y

$$\rho\left(u\frac{\partial v}{\partial x} + v\frac{\partial v}{\partial y}\right) = -\frac{\partial p}{\partial y} + \mu\left(\frac{\partial^2 v}{\partial x^2} + \frac{\partial^2 v}{\partial y^2}\right) \tag{II.5}$$

Energy Equation

$$\rho c_p\left(u\frac{\partial T}{\partial x} + v\frac{\partial T}{\partial y}\right) = k\left(\frac{\partial^2 T}{\partial x^2} + \frac{\partial^2 T}{\partial y^2}\right) + \rho D\left(c_{pv} - c_{pa}\right)\left(\frac{\partial T}{\partial x}\frac{\partial W}{\partial x} + \frac{\partial T}{\partial y}\frac{\partial W}{\partial y}\right) \tag{II.6}$$

The second term of the right part of this equation (II.6) which represents the heat transfer by inter-diffusion is considered as negligible comparing to the first term (Yan et al. [34]). So, this equation becomes:

$$\rho c_p \left(u\frac{\partial T}{\partial x} + v\frac{\partial T}{\partial y} \right) = k\left(\frac{\partial^2 T}{\partial x^2} + \frac{\partial^2 T}{\partial y^2} \right) \tag{II.7}$$

Mass-Diffusion Equation

$$u\frac{\partial W}{\partial x} + v\frac{\partial W}{\partial y} = D\left(\frac{\partial^2 W}{\partial x^2} + \frac{\partial^2 W}{\partial y^2} \right) \tag{II.8}$$

II.4.2 Dimensionless equations

To give a general formulation to the problem, we transform the governing equations under their dimensionless form by adopting the following dimensionless quantities:

$$X = \frac{x}{2H} \quad ; \quad Y = \frac{y}{2H} \quad ; \quad U = \frac{u}{u_{in}} \quad ; \quad V = \frac{v}{u_{in}}$$

$$\theta = \frac{T - T_{in}}{T_w - T_{in}} \quad ; \quad C = \frac{W - W_{in}}{W_w - W_{in}} \quad ; P = \frac{p}{\rho_{in}u_{in}^2}$$

After including the dimensionless quantities, the equations (II.3)-(II.8) can be written:

$$\frac{\partial U}{\partial X} + \frac{\partial V}{\partial Y} = 0 \tag{II.9}$$

$$U\frac{\partial U}{\partial X} + V\frac{\partial U}{\partial Y} = -\frac{\partial P}{\partial X} + \frac{2}{Re}\left(\frac{\partial^2 U}{\partial X^2} + \frac{\partial^2 U}{\partial Y^2} \right) \tag{II.10}$$

$$U\frac{\partial V}{\partial X} + V\frac{\partial V}{\partial Y} = -\frac{\partial P}{\partial Y} + \frac{2}{Re}\left(\frac{\partial^2 V}{\partial X^2} + \frac{\partial^2 V}{\partial Y^2} \right) \tag{II.11}$$

$$U\frac{\partial \theta}{\partial X} + V\frac{\partial \theta}{\partial Y} = \frac{2}{Re\,Pr}\left(\frac{\partial^2 \theta}{\partial X^2} + \frac{\partial^2 \theta}{\partial Y^2} \right) \tag{II.12}$$

$$U\frac{\partial C}{\partial X} + V\frac{\partial C}{\partial Y} = \frac{2}{Re\,Sc}\left(\frac{\partial^2 C}{\partial X^2} + \frac{\partial^2 C}{\partial Y^2} \right) \tag{II.13}$$

II.4.3 Dimensionless numbers characterizing the problem

In the dimensionless equations of the previous paragraph, other dimensionless numbers take place. These numbers are defined as follows:

- **Aspect ratio**: It is the ratio between the width and the length of the channel.

$$\gamma = \frac{2H}{L} \tag{II.14}$$

- **Reynolds number:** It represents the ratio between the inertial force and the viscous force.

$$Re = \frac{u_{in}D_h}{\nu} \tag{II.15}$$

With $D_h = 4.H$

- **Prandtl number:** It represents the ratio between the rate of diffusion of viscous effect and the rate of diffusion of heat.

$$Pr = \frac{\nu}{\alpha} \tag{II.16}$$

- **Schmidt number:** It represents the ratio between the rate of diffusion of viscous effect and the rate of diffusion of mass.

$$Sc = \frac{\nu}{D} \tag{II.17}$$

- **Friction factor:** It measures the friction of the fluid on the channel wall.

$$f.Re = 4\frac{\partial U}{\partial y}\Big|_{y=0} \tag{II.18}$$

The heat flux changed in the vicinity of the wet wall is made up of two types of heat:

    ○ Sensible heat: transferred energy to the liquid under the effect of the temperature gradient. Neglecting the energy transferred by radiation, the expression of this heat is given by:

$$q''_s = -k \frac{\partial T}{\partial y}\bigg|_{y=0} \tag{II.19}$$

Where k is the thermal conductivity of the mixture.

    ○ Latent heat: transferred energy to the mixture to change the vapor state to liquid, its expression of this heat is given by:

$$q''_l = \frac{\rho D h_{fg}}{1 - W_w} \frac{\partial W}{\partial y}\bigg|_{y=0} \tag{II.20}$$

The total transferred heat flux is:

$$q'' = q''_s + q''_l = -k \frac{\partial T}{\partial y}\bigg|_{y=0} + \frac{\rho D h_{fg}}{1 - W_w} \frac{\partial W}{\partial y}\bigg|_{y=0} \tag{II.21}$$

- **Sensible Nusselt number:** It provides a comparison between the flux transferred by thermal convection and that transferred by conduction. It is given by the following expression:

$$Nu_s = -\frac{2}{1 - \theta_m} \frac{\partial \theta}{\partial Y}\bigg|_{Y=0} \tag{II.22}$$

With: $\theta_m = \frac{1}{U_m} \int_0^1 U \, \theta \, dY$

- **Latent Nusselt number:** It is ratio between the flux transferred by mass convection and that transferred by conduction.

$$Nu_L = -\frac{2S}{(1 - \theta_m)(1 - w_w)} \frac{\partial C}{\partial Y}\bigg|_{Y=0} \tag{II.23}$$

Where S is a factor which indicates the importance of heat due to the mass diffusion against that due to thermal diffusion. Its expression is given by: [Lee et al. [35]]:

$$S = \rho D h_{fg}(W_w - W_{in})/k(T_w - T_{in}) \tag{II.24}$$

The combination of these two numbers (Nu_s and Nu_L) gives the total Nusselt number (Ait Hammou [15]):

$$Nu_T = Nu_s + Nu_L \tag{II.25}$$

So,

$$Nu_T = \frac{h_m D_h}{k} = \frac{q''_T D_h}{[k(T_w - T_m)]} \tag{II.26}$$

• **Sherwood number:** It is the ratio between the flux transferred by mass convection and that transferred by mass diffusion. It is defined by the relation:

$$Sh = \frac{h_m D_h}{D} = \frac{\dot{m}''}{\rho(W_w - W_m)} \frac{D_h}{D}$$

The condensed mass flux is given by:

$$\dot{m}'' = \rho_L v_L = W_w \rho v_e - \rho D \frac{\partial W}{\partial y}\Big|_{y=0} \tag{II.27}$$

So, Sherwood number is:

$$Sh = \frac{-D_h}{(1 - W_w)(W_w - W_m)} \frac{\partial W}{\partial y}\Big|_{y=0} \tag{II.28}$$

Since w_w stay small in this study, this expression can be simplified as follows:

$$Sh = \frac{-D_h}{(W_w - W_m)} \frac{\partial W}{\partial y}\Big|_{y=0} \tag{II.29}$$

The corresponding dimensionless form is:

$$Sh = \frac{-2}{(1 - C_m)} \left. \frac{\partial C}{\partial Y} \right|_{Y=0} \tag{II.30}$$

II.4.4 Boundary conditions

The boundary conditions are the conditions imposed on the walls, the inlet and the outlet of the channel. These conditions are given by their dimensionless form such as:

a. At the inlet $(X = 0, \ 0 < Y < 1)$

$$U = 1 \text{ and } V = C = \theta = 0 \tag{II.31}$$

b. The left wall $\left(Y = 0, \ 0 < X < {}^{1}\!/_{\gamma}\right)$

$$U = 0, \qquad C = \theta = 1 \ V = V_e \tag{II.32}$$

c. The right wall $\left(Y = 1, \ 0 < X < {}^{1}\!/_{\gamma}\right)$

$$U = 0 \quad ; \quad V = 0 \tag{II.33}$$

$$\left. \frac{\partial \theta}{\partial Y} \right|_{Y=1} = 0 \quad ; \quad \left. \frac{\partial C}{\partial Y} \right|_{Y=1} = 0 \tag{II.34}$$

d. The outlet $(X = {}^{1}\!/_{\gamma}), \ 0 < Y < 1$

$$\frac{\partial V}{\partial X} = \frac{\partial U}{\partial X} = \frac{\partial \theta}{\partial X} = \frac{\partial C}{\partial X} = 0 \tag{II.35}$$

Where V_e is the condensation velocity of water estimated by Lee et al. [35]:

$$V_e = -\frac{2}{Re \ Sc} \frac{W_w - W_{in}}{1 - W_w} \left. \frac{\partial C}{\partial Y} \right|_{Y=0} \tag{II.36}$$

This velocity is deduced for a steady state flow with a small variation of the film thickness along the plate and it is recalculated each iteration.

In order to use the transverse velocity in the mass flow rate calculation, we transform the equation (II.36) to be:

$$V_{ed} = -2\frac{D}{D_h}\frac{W_w - W_{in}}{1 - W_w}\frac{\partial C}{\partial Y}\bigg|_{Y=0} \tag{II.37}$$

The condensed mass flow rate per unit width is related to the condensation velocity by:

$$\dot{m} = \rho V_{ed}\, dx \tag{II.38}$$

II.5   Conclusion

In this chapter, we have presented the physical model, followed by the simplifying assumptions and the mathematical model, including the governing equations and the boundary conditions. The next chapter will include the solution method, the grid independence and a series of validation tests.

Chapter III

NUMERICAL SOLUTION

III.1   Introduction

In this chapter, we present the description of the solution method used to solve the conservation equations that govern the problem, the grid independence and the validation procedure of the computer code.

III.2   Solution method description

Since it is impossible to solve the equations system that describes the transfer of quantities analytically, several numerical methods have been developed. We can mention as an example: finite difference method, finite volume method, finite element method. These methods allow transforming the partial derivative equation system to algebraic equation system.

In our study, the solution of the partial differential equations modeling the flow field and heat-mass transfers is based on the finite volume method.

The velocity-pressure coupling is treated with the SIMPLER algorithm (Patankar [36], 1980), with a power law scheme for the convective fluxes and central scheme for the diffusion fluxes. An overview about this method is presented.

A partial derivative equation of a dependent variable **Φ** is presented like this:

$$\frac{\partial(\rho\Phi)}{\partial t} + \frac{\partial(\rho u_i \Phi)}{\partial t} = \frac{\partial}{\partial x_i}\left(\Gamma \frac{\partial\Phi}{\partial x_i}\right) + S \quad ....(\text{III-1})$$

To find the equations that govern heat and mas transfer in our problem, we present in the following table the values of **Φ, S** and **Γ.**

Table III.1: Values of **Φ, S** and **Γ** correspond to governing equations

Equation	**Φ**	**Γ**	**S**
Continuity	1	0	0
Momentum Quantity following X	U	2/Re	0
Momentum Quantity following Y	V	2/Re	0
Energy	θ	2/Pr Re	0
Concentration	C	2/Sc Re	0

The solution of equations similar to equation (III-1) using finite volume method goes through the discretization in each cell, called control volume (Fig.III.1), integral form of the being resolved equations instead of their differential form(Patankar [36]).
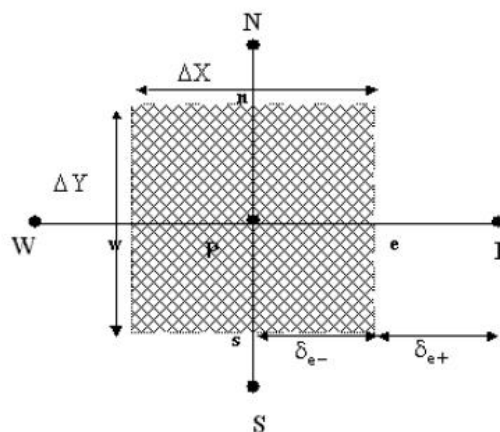

Figure III.1: Principal control volume scheme

The discretized equations are obtained by integration of equation (III.1) around each control volume schematized in the figure (III.1) .The coupling between the continuity

and the momentum quantity equations requires a specific treatment. For that, we are going to use the staggered grid to evaluate the velocity field (Figure III.2). The principal grid will be reserved for the scalar variables (pressure, temperature and concentration).
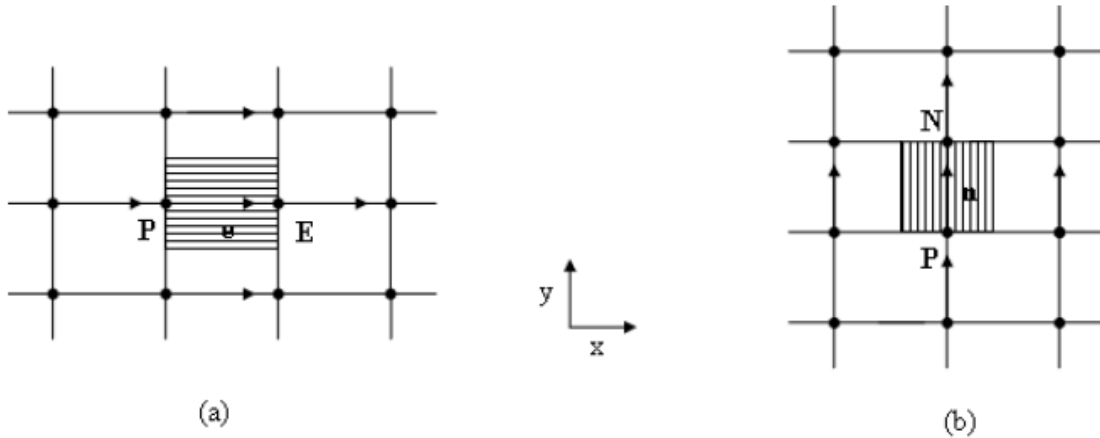

(a)   (b)

Figure III.2: Grid scheme (a) staggered grid to the right (b) staggered grid to the left.

The discretization of the momentum quantity equation is found by integration of equation (III.1) by replacing **Φ** by u and/or v. After simplifying, we find:

$$a_e u_e = \sum_n a_{nb} u_{nb} + b_u + A_e(P_P - P_E) \quad ....(III.2)$$

$$a_e v_e = \sum_n a_{nb} v_{nb} + b_v + A_e(P_P - P_N) \quad ....(III.3)$$

The coupling between the momentum quantity equations and the continuity equation causes a problem, of the fact that the calculated velocity field using momentum quantity equation does not satisfy the continuity equation. To exceed such a problem, Patankar has developed an algorithm called SIMPLER, the latter consists in giving estimation about pressure field and calculating the velocity field. As this velocity field does not satisfy the continuity equation, an iterative computation that allows correcting this field is required until the continuity equation is satisfied.

The equations of discretization for the other scalar variables are obtained by taking in the discretized equation, the temperature as a variable for the energy equation and the concentration for the concentration equation.

The SIMPLER Algorithm can be summarized in the following steps:

1. Guessed velocity field.

2. Calculate coefficients for the momentum equations then calculate the pseudo velocity.

3. Calculate coefficients for the pressure equation then solve it.

4. Solve the momentum equations using the previous pressure field.

5. Solve the correction pressure equation p'.

6. Correct the velocity field. (But do not correct the pressure).

7. Solve the discretization equation for other **Φ**'s.

8. Convergence test.

If the test is not satisfied: return to step 2 using the new field p as an estimation field.

The discretized equations solution requires an iterative computation because of the nonlinearity and the coupling between them. Then, during the solution of the variable equation, the other variables are considered constant and their values are equal to the one of the previous iteration. This procedure is repeated until the convergence of all the variables. The convergence criterion of the iterative procedure is based on the relative error, where is must be less than 10^{-5} (relative error = $(\boldsymbol{\Phi}_{i,j}^{n+1} - \boldsymbol{\Phi}_{i,j}^{n})/\boldsymbol{\Phi}_{i,j}^{n+1}$).

III.3 Grid independence

In order to balance between the precision of the results and achieving the convergence in a minimum time, a study about grid independence has been carried out. The nonuniform grid has been used in both the stream-wise and transverse directions, with greater node density near the inlet and the walls where the gradients are expected to be more significant. To check the adequacy of the numerical scheme and the constructed code, the results for the case of forced heat convection were obtained. Two Different grids (100 x 45 and 200 x 90) were considered to establish the grid independence. The results of this study are obtained by comparing the values of Friction factor, Nusselt number and Sherwood number. The tables III.2 show that the results differ by less than 2%.

Since the increase of the number of nodes by a factor of four (from 100 × 35 to 200 × 90) results in changes of less than 2% on the values of the Nusselt number, Sherwood number and friction coefficient (changes achieve 2% in the inlet vicinity due to high gradient, where it is 0.04% at the outlet for Nusselt and Sherwood numbers, and 0.33%

for the friction coefficient), the 100×45 discretization was deemed to be sufficiently accurate. All the results presented in this study have therefore been calculated using 100 and 45 nodes in the X and Y directions, respectively.

The grid sensitivity tests are presented for the following conditions:

$$Re=300; T_w=20\ ^\circ C; T_{in}=40^\circ C;\ \varphi_{in}=10\%, \gamma=1/65.$$
$$Sc=0.58; Pr=0.7.$$

Table III.2: Effects of discretization on calculated results

X	$f * Re$		Nus		Sh	
	100*45	200*90	100*45	200*90	100*45	200*90
0.7	40.55	41.31	11.36	11.47	10.77	10.86
1.01	36.2	35.8	9.96	9.92	9.43	9.37
2.96	26.85	27.3	6.80	6.81	6.47	6.48
15	23.97	24.03	5.01	4.99	4.95	4.93
65	24.04	24.12	4.852	4.854	4.853	4.855

III.4 Computer code validation

To ensure the validity of the computer code, we have compared our result with some published results. The validation of it has been carried out in two steps. First, the calculated axial evolution of the friction factor, average temperature and Nusselt number for hydrodynamically and thermally developing forced convection was very close with corresponding published results [15]. Then, the calculated axial evolution of Sherwood number for thermal flow with mass transfer shows an excellent agreement between our results and that published in [15].

III.4.1 Hydrodynamically and thermally developed forced convection

In order to check the validity of the developed code, we have applied it to a problem of heat transfer, for the case of a forced flow; the thermophysical properties are calculated according to one third rule. The gas mixture flows through a vertical channel of two

isothermal plates. Dynamic and thermal parameters have been chosen to ensure the correctness of solving hydrodynamic and thermal flow. The obtained results about the axial evolution of the friction factor, average temperature and Nusselt number in the left isothermal plate are compared to the ones of Ait Hammou et al [15] (2004), for the following conditions: Re=300; T_w=20; T_{in}=40; φ_{in} =10%, γ=1/65.

The figures III.3 and III.4 and III.5 show the comparison between our results and Ait Hammou's (2004). The relative differences are gathered in the tables III.3, III.4 and III.5.
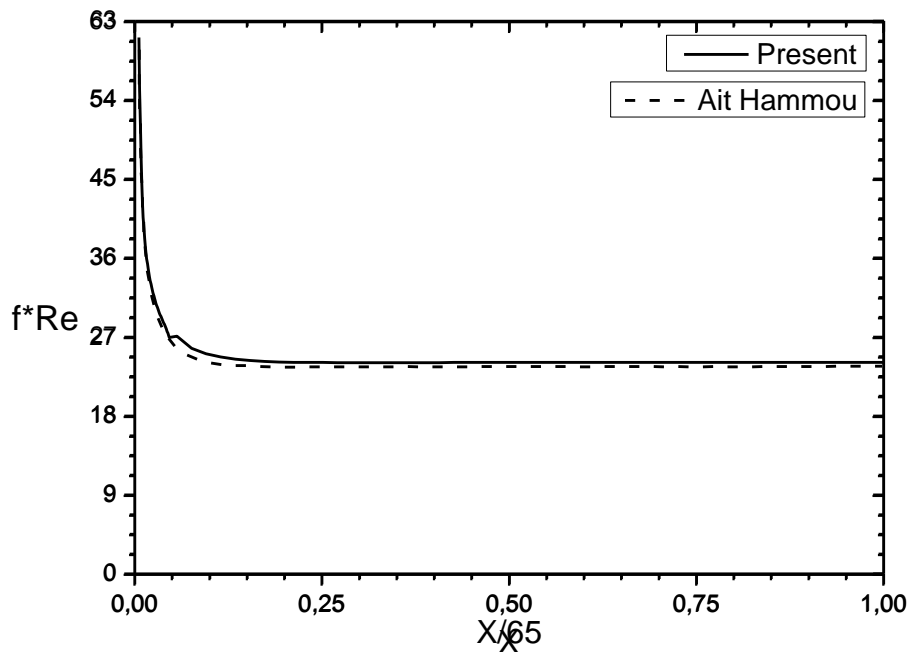

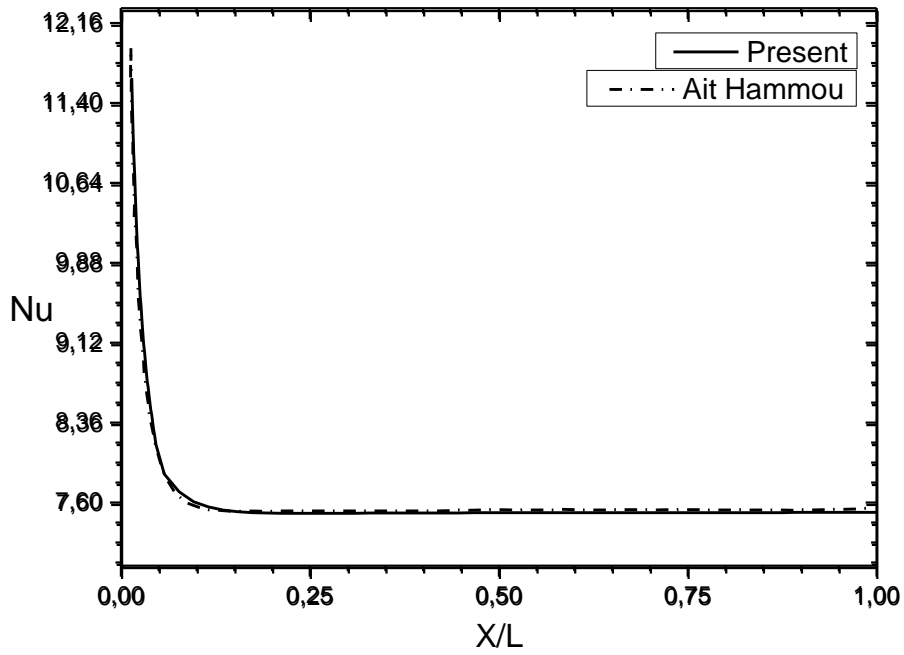**Figure III.3**: Axial evolution of the friction factor
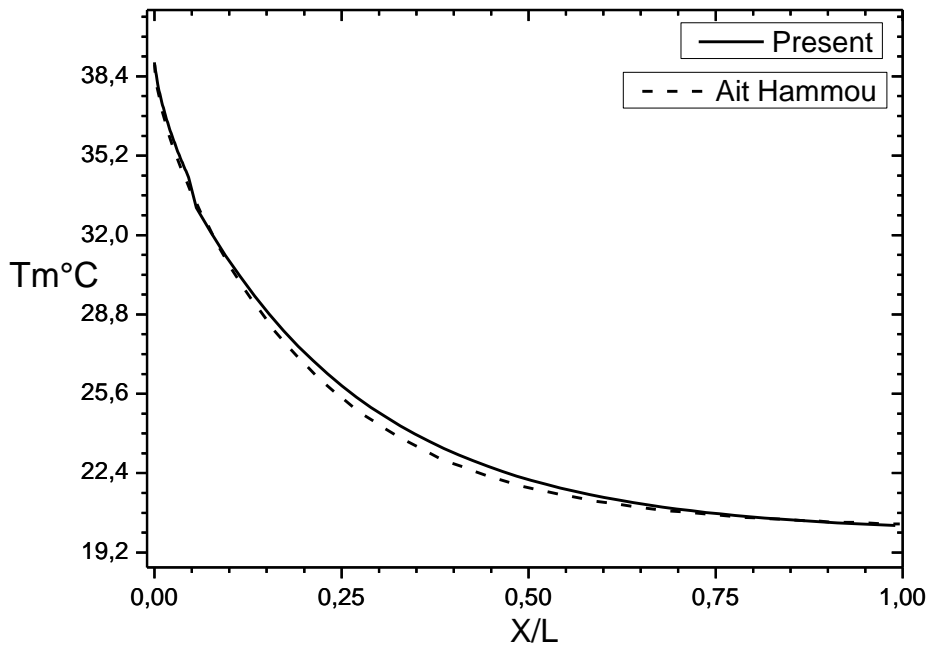
Figure III.4: Axial evolution of Nusselt number

Figure III.5: Axial evolution of average temperature

Table III.3: Validation of the friction factor

X/65	0.11	0.21	0.5	1
Our results	24.67	24.08	24.06	24.07
Ait Hammou's result	23.92	23.55	1.91	1.49
Relative difference (%)	2.9	1.99	1.91	1.49

Table III.4: Validation of the sensible Nusselt number.

X/65	0.016	0.21	0.5	1
Our results	10.74	7.520	7.526	7.528
Ait Hammou's result	10.74	7.521	7.532	7.543
Relative difference (%)	0	0.01	0.08	0.2

Table III.5: Validation of the average temperature.

X/65	0.003	0.1	0.5	1
Our results	38.25	30.75	22.1	20.28
Ait Hammou's result	38.04	30.57	21.81	20.35
Relative difference (%)	0.55	0.58	1.31	0.34

After comparison between our results and the ones of Ait Hammou (Ait Hammou et al. [15]) (Table III.3), for the friction factor, it's noted that the maximum relative difference is less than 3%, which is due to the imprecision associated with the digitization of their graphical results.

For the average temperature (Table III.5), we note a very good agreement where the difference doesn't exceed 2%. This small difference is due to the imprecision associated with the digitization of their graphical results, as well.

About Nusselt number (Table III.4), we note an excellent agreement between our results and Ait Hammou's, where the relative difference is less than 1%.

The agreement between our results and those of Ait Hammou [15] ensures the validity of our code to compute for such a flow type.

III.4.2 Thermal flow with mass transfer

For another test, the validation has been done to ensure the validity of the results obtained for the solution of energy and concentration equations. The comparison is carried out with the results of Hammou et al [15] for developing thermal flow with mass transfer.

In order to make sure that the solution of concentration equation is true, a mass transfer parameter has been chosen. The obtained results about the axial evolution of the Sherwood number in the left isothermal plate are compared to the ones of Ait Hammou et al [15][2004], for the following conditions:

$$Re = 300; T_w = 20 \text{ °C} ; T_{in}=40 \text{ °C} ; \varphi_{in} = 10\%, \gamma=1/65,$$

$$Sc = 0.58 , Pr = 0.7.$$

The figure III.6 illustrates the comparison between our results and Ait Hammou's [15]. The relative difference is shown in the table III.6.
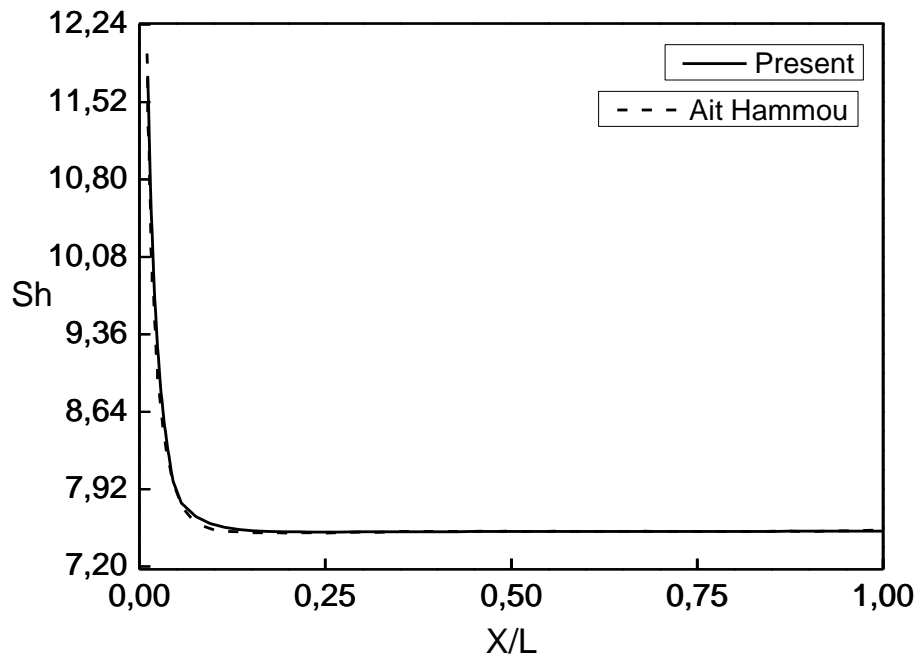
Figure III.6: Axial evolution of Sherwood number.

Table III.6: Validation of Sherwood number.

X/65	0.015	0.25	0.6	1
Our results	10.49	7.522	7.527	7.52
Ait Hammou's result	10.43	7.511	7.526	7.54
Relative difference(%)	0.58	0.15	0.01	0.26

An excellent agreement is shown between the two results for Sherwood number, where the relative difference is less than 1%. The agreement between our results and those of Ait Hammou ensures the validity of our code to compute for a flow with heat and mass transfer.

The above figures and discussion show that for the most part, the present model agrees well with Ait Hammou's results and the discrepancies found in some cases are likely due to the imprecision associated with the digitization of graphical results.

In view of these successful comparisons, we conclude that the computer code is reliable and can be used to analyze the problem under consideration.

III.5 Conclusion

In this chapter, we have presented the numerical method used to solve the discretized equations, the grid independence test and a series of validation tests.

These validation tests show that our computation code   is valid and that we can simulate the flows for forced convection with heat and mass transfer.

Chapter IV

RESULTS AND DISCUSSION

IV.1   Introduction

This chapter presents results from the application of the present model to condensation of steam-air mixture. A wide range of input parameters has been used to study the condensation process inside channels. A mixture of steam and air was chosen because it is by far the most common combination of a condensing vapor with a noncondensable gas. The steam-air mixture flows through a vertical channel with parallel plates.

The presented numerical simulations in this chapter have been encompassed for a better understanding of the condensation process of the water vapor contained in the warm air on an isothermal plate in a vertical channel for laminar flow in case of forced convection.

The mixture temperature, the Reynolds number (or the velocity) and the relative humidity characterize the inlet conditions. As mentioned earlier, these variables are

assumed to be uniform across the inlet. The variable ΔT defines the temperature difference between the inlet mixture and the condensing plate.

The effect of each inlet parameter is studied by examining the mass flow rate and heat transfer along the channel.

This chapter includes four parts. The first part concerns the evolution of the average temperature and concentration, in addition to the effect of different parameters (T_{in}, Re_{in}, φ_{in}) on them. The second one relates to the evolution of the temperature and the concentration on the adiabatic wall. In the third part however, interests in the axial evolution of sensible, latent Nusselt and Sherwood numbers will be presented as function of different parameters such as inlet relative humidity, Inlet Reynolds number and the aspect factor. The effect of inlet parameters (T_{in}, Re_{in} and φ_{in}) and the aspect ratio on both the total and axial evolution of the condensed mass flow rate will be the concern of the last part.

In order to ensure a downward flow, we have considered the boundary conditions illustrated in figure II.1. The left wall wetted with a thin liquid film and maintained at a constant temperature T_w which is lower than that of the steam-air mixture inlet temperature T_{in}.

IV.2   Axial evolution of average temperature and concentration

The rate of humid air cooling during its passageway through the channel can be determined by its mixture average temperature T_m. The axial evolution of the average temperature is presented in figure (IV.1). This figure shows that T_m decreases as the mixture gets ahead the channel. This reduction, which expresses a cooling of the air, is due to the sensible heat transferred from the humid air to the isothermal wall. A careful examination of figure (IV.1) shows that as Reynolds increases at the channel inlet, the humid air cooling becomes weak. It is noteworthy that the condensation of water vapor contained in the air, which is more important for Re = 900 (See figures IV.20 and IV.21), plays an important role in the behavior of T_m for different values of Reynolds number. Indeed, the humid air cooling is lower in the case of Re = 900 because the water vapor condensation releases the latent heat which is absorbed by the air flow [Kassim [32]].
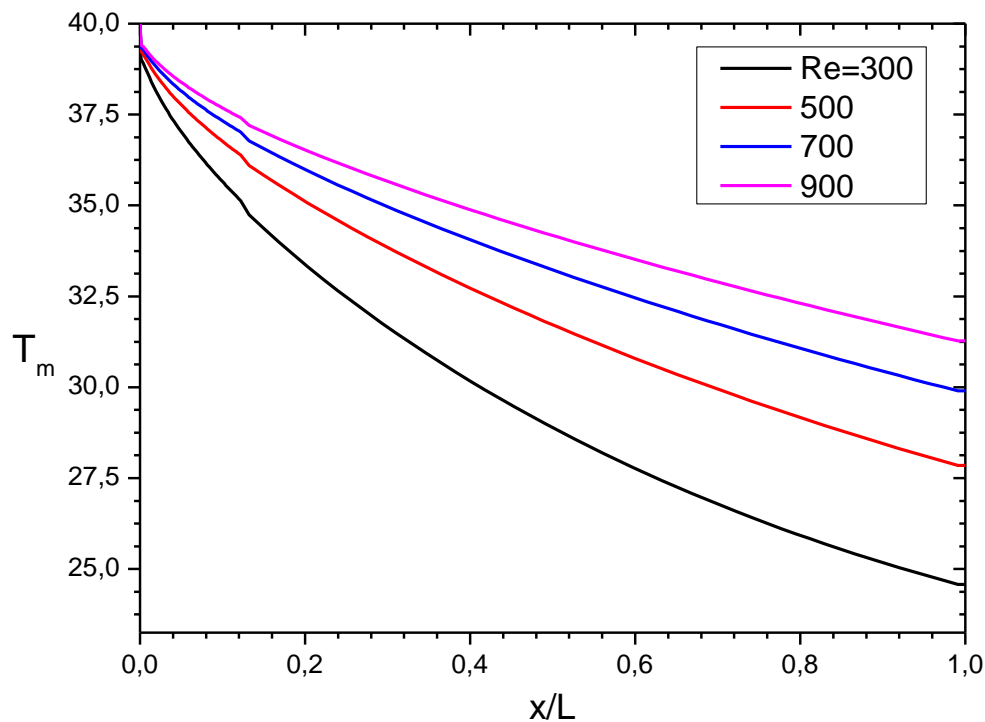

Figure IV.1 : Axial evolution of average temperature for different values of inlet Reynolds number

The axial evolution of the mixture concentration, W_m, along the channel is presented in figure (IV.2). We notice that for all the cases, W_m decreases as the air penetrates the channel. This decrease is due to the condensation of the vapor contained in the humid air. For different values of Reynolds number, W_m takes lower values when Reynolds

number is reduced; this is explained by a rise of mass transfer. We note that there is no convergence in the outlet for the presented cases.

Figure (IV.3) shows the axial evolution of the average concentration W_m. We can see that W_m rises for the case of φ_{in} = 10%, and decreases for the other cases (φ_{in} =40 and φ_{in} 60%). The rise of W_m for φ_{in} = 10% is due to the liquid film evaporation; the latter happens even when the wall temperature is lower than the inlet one because the inlet concentration (which corresponds to the inlet temperature) is less than the wall's for this inlet humidity (see table (IV.1)). On the other hand, for the two other cases (φ_{in} =40 and φ_{in} 60%), condensation takes place. For the condensation case, where the vapor concentration at the channel inlet is higher than that of the wall, the average concentration rises with the increase of inlet humidity.

Table IV.1: Values of parameters of the study

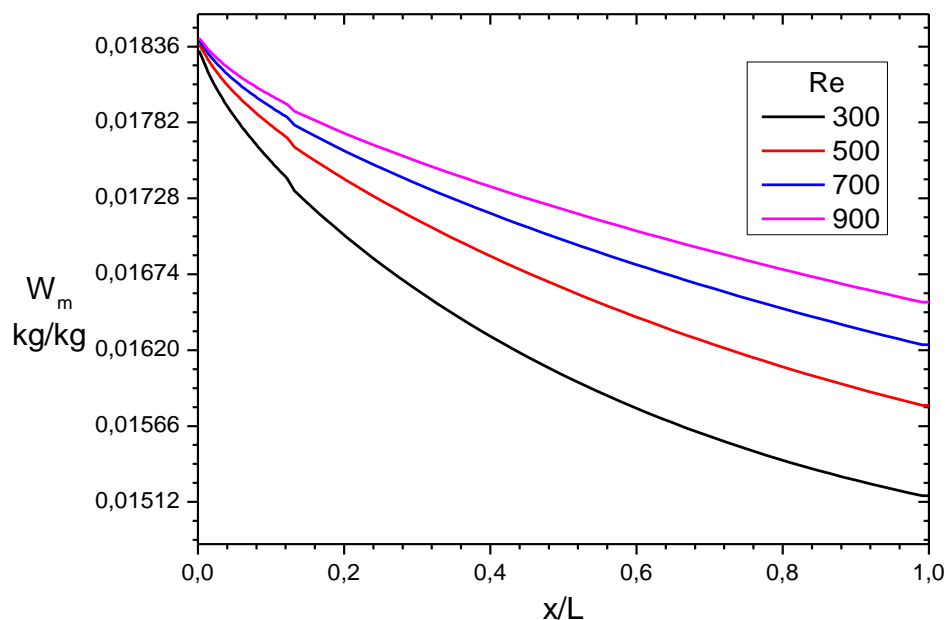|	T_{in} (°C)	φ_{in} (%)	W_{in} (g/kg)	T_w (°C)	W_w (g/kg)
Case I	40	10	4.598	20	14.9
Case II	40	40	18.547	20	14.9
Case III	40	60	27.979	20	14.9

Figure IV.2: Axial evolution of average concentration for different values Re
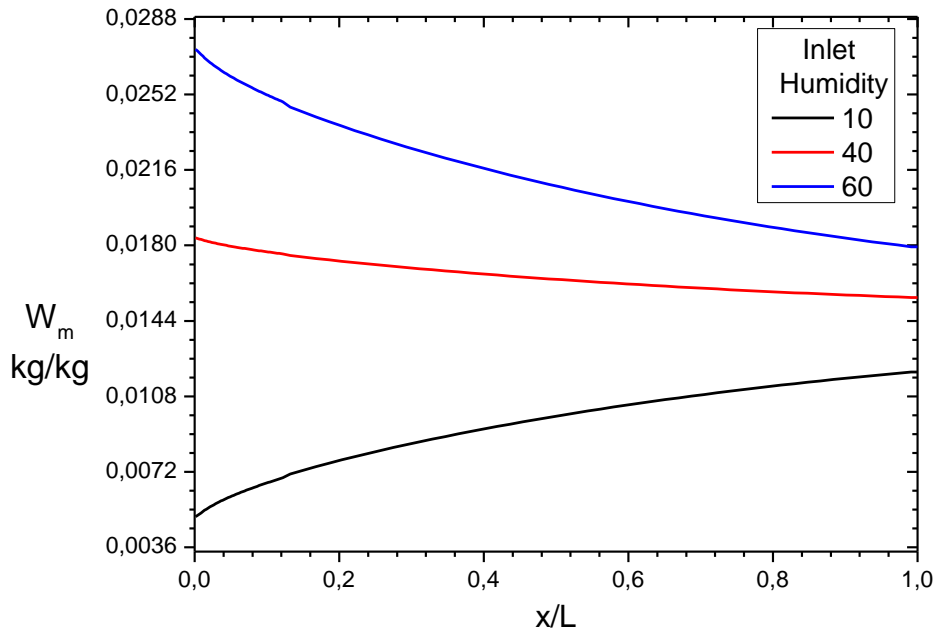
Figure IV.3: Axial evolution of average concentration for different values of inlet relative humidity

IV.3 Axial evolution of concentration and temperature on the adiabatic wall

To study the effect of the channel inlet relative humidity of the humid air flow on the heat and mass transfer, we present the results of the numerical simulation for three different values of the air humidity. The studied channel (figure (II.1)) is formed of two vertical parallel plates of length L and width $2h=1/65$ ($\gamma=1/65$).

Figure (IV.4) shows the axial evolution of the mass fraction W_{adia} on the adiabatic wall. We note that W_{adia} increases slightly for φ_{in} = 10% where it decreases in the other cases. Indeed, since the adiabatic wall is dry, its mass fraction is the one taken by the air in the channel inlet and it decreases as the air penetrates through the channel for φ_{in} = 40% and 60% while it increases for φ_{in} = 10%. We note, moreover, that for φ_{in} = 10% (W_{in}= 4.598 g/kg) the vapor mass fraction is less than that of the liquid film (W_w = 14.9 g/kg) leading to the evaporation. On the other hand, for the two other cases, φ_{in} = 40% and 60%, the vapor mass fraction is higher than that of the wall (see table (IV.1)), so the water vapor contained in the air condenses on the wet wall. The condensation becomes more and more important when φ_{in} rises.
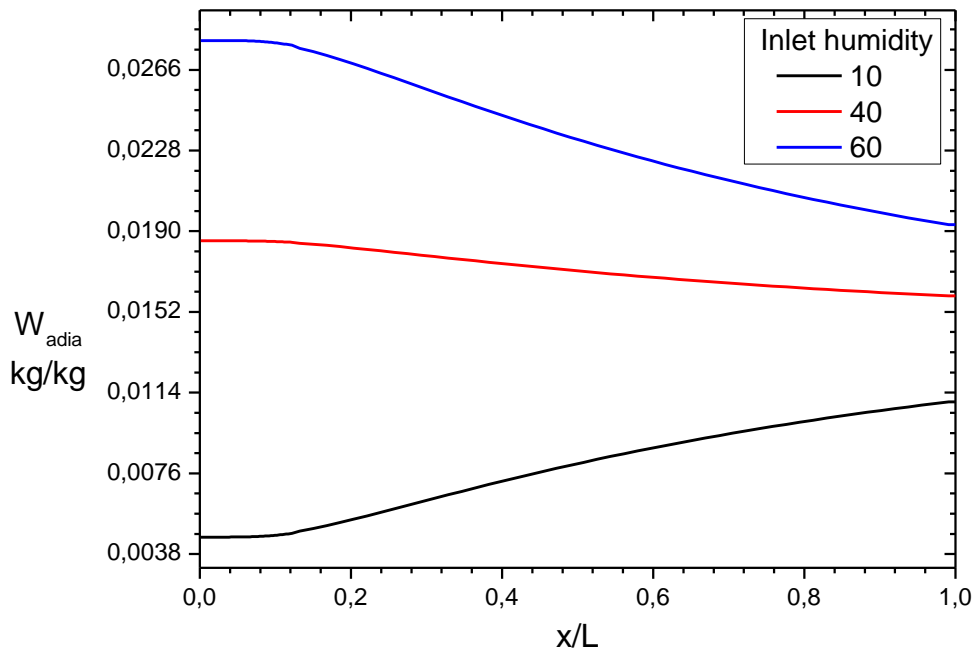
Figure IV.4: Axial evolution of concentration on the adiabatic wall for different values of inlet relative humidity.

The axial evolution of the concentration on the adiabatic wall, W_{adia}, for different values of Reynolds number is shown in figure (IV.5). We notice that W_{adia} decreases and takes values included between 18.547 g/kg and 14.9 g/kg, which corresponds respectively to that of humid air at inlet, and that taken in the wet wall. In fact, since the adiabatic wall is dry, its mass fraction is that taken at the channel inlet. The reduction of the concentration on the adiabatic wall is due to the mass transfer from the adiabatic wall vicinity to the wet wall because of the condensation phenomenon. At a given axial position, it is observed that the rise of Reynolds number reduces the mass transfer from the adiabatic wall to the wet wall.
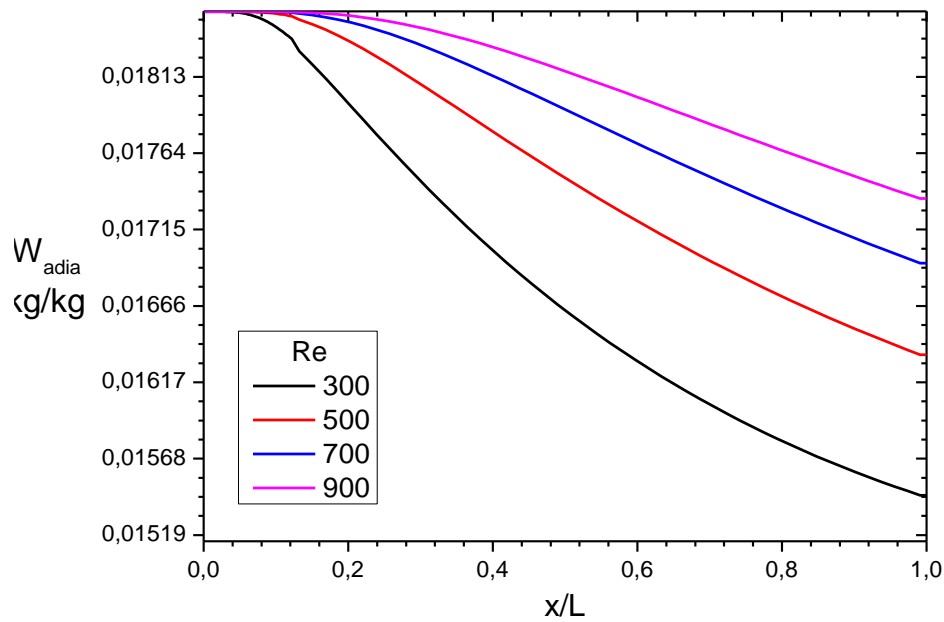
Figure IV.5: Axial evolution of concentration on the adiabatic wall for different values of inlet Reynolds number.

The axial evolution of the temperature on the adiabatic wall is presented in figure (IV.6). knowing that this temperature is that of the humid air flow at its vicinity, it is obvious that T_{adia} decreases as the humid air penetrates through the channel. This decrease is due to a transfer by sensible heat from the flowing air to the isothermal wall.
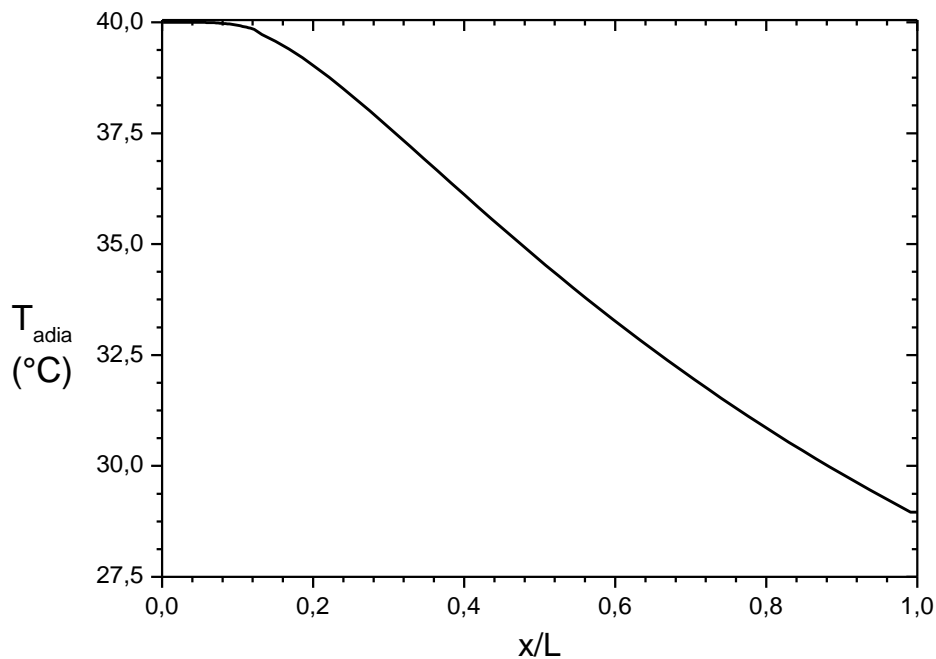

Figure IV.6: Axial evolution of temperature on the adiabatic.

Figure (IV.7) depicts the axial evolution of the adiabatic wall temperature for different values of Reynolds number. We note that T_{adia} decreases and presents a similar trend as T_m. As it is mentioned above, the decrease of T_{adia} is due to a sensible heat transfer from the adiabatic wall to the wet one which comes to cool it. Moreover, we note that the cooling of the adiabatic wall declines with the increase of Reynolds number. This is due to the rise of the latent heat transfer from the film, which heats the adiabatic wall (see figure IV.12).
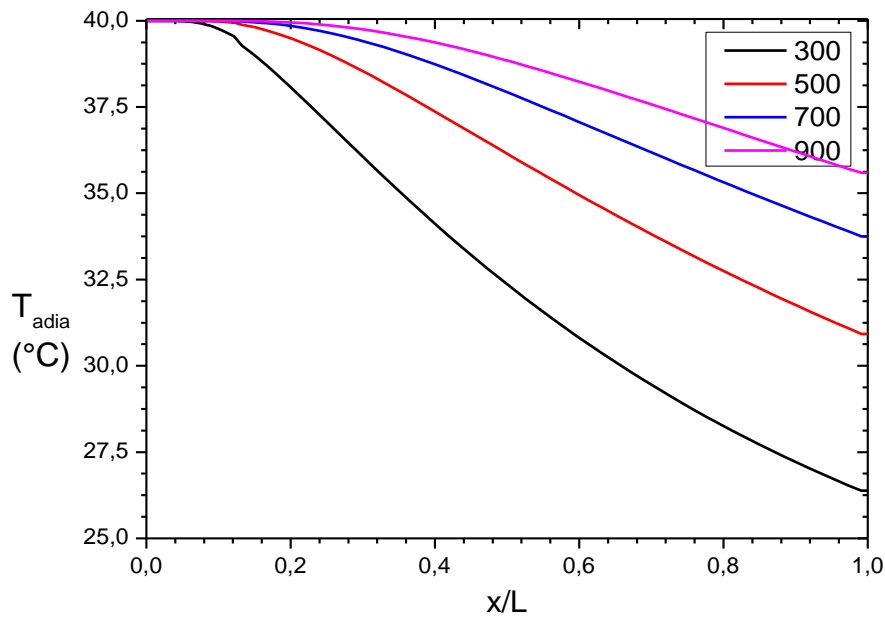

Figure IV.7: Axial evolution of temperature on the adiabatic wall for different values of inlet Reynolds number.

IV.4   Axial evolution of sensible and latent Nusselt numbers

Figure (IV.8) presents the axial evolution of the sensible Nusselt number on the isothermal wall. The Nu_s evolution is plotted using the following data: Tin = 40 °C, φ_{in} = 40 % (W_{in} = 18.547 g/kg), T_w (°C) = 20 °C (W_w = 14.9 g/kg) and Re=400. This wall is wet with a thin liquid film and maintained at a temperature T_w = 20 °C, which is less than the flowing humid air temperature at the inlet of the channel (Tin=40 °C) so the flowing air is cooled. We note that Nu_s decreases sharply until the channel outlet where it takes an asymptotic value. This asymptotic value (4.86) corresponds to that of a fully developed value for forced convection [Shah and London [37]; Bejan [38]].
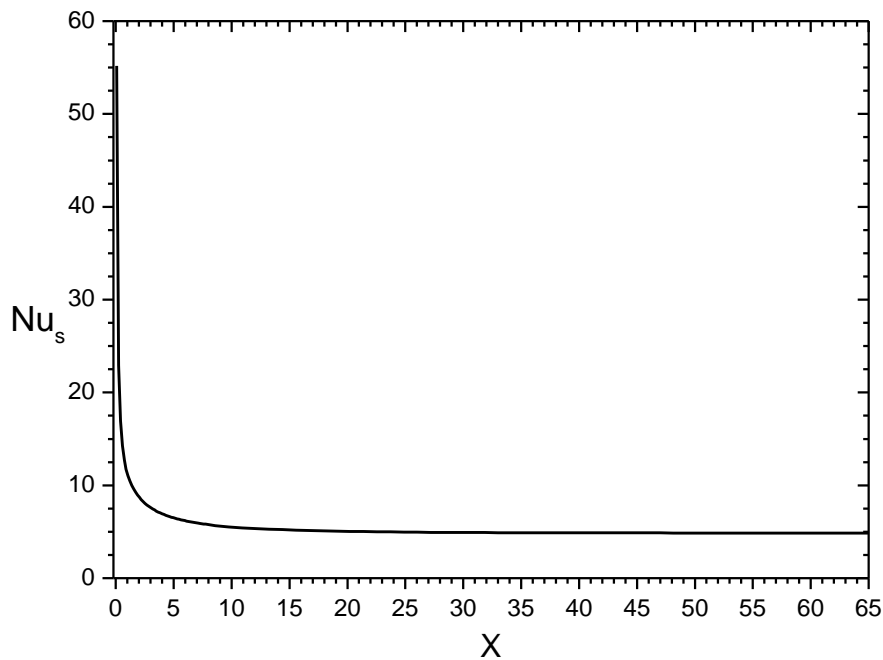
Figure IV.8: Axial evolution of the sensible Nusselt number

The axial evolution of the latent Nusselt number, Nu_L, along the channel is shown in the figure (IV.9). This number provides the rate of the heat change by condensation (for condensation case) between the flowing air and the liquid film. Indeed, at the channel inlet vicinity Nu_L decreases in a similar way as Nu_s and Sh, presenting a substantial reduction, then it tends to an asymptotic value. This means that the great amount of heat transfer happens et the inlet vicinity. We notice that the latent Nusselt number has negative values for $\varphi_{in} = 10\%$, while it takes positive values for $\varphi_{in} = 30\ \%$ and 60%. For the case of $\varphi_{in} = 10\%$, evaporation takes place because the concentration at the wall is higher than that of the inlet ($T_w = 20°C$ so $C_w = 14.9$ g/kg; $T_{in} = 40\ °C$ and $\varphi_{in} = 10\ \%$ so $W_{in} = 7.37$ g/kg), see table (IV.2). For the two other cases ($\varphi_{in} = 30\ \%$ and 60 %), condensation takes place. We note that for the condensation case, Nu_L becomes more important when the inlet relative humidity increases, this is due to the rise of difference between the concentration at the inlet and that of the wall. On the other hand, this confirms the resistance made by the noncondensable gas which reduces the transfer when its concentration increases. Table (IV.2) presents the values of concentration at the channel inlet for different values of inlet relative humidity.

Table IV.1: Inlet concentration for different values of inlet relative humidity

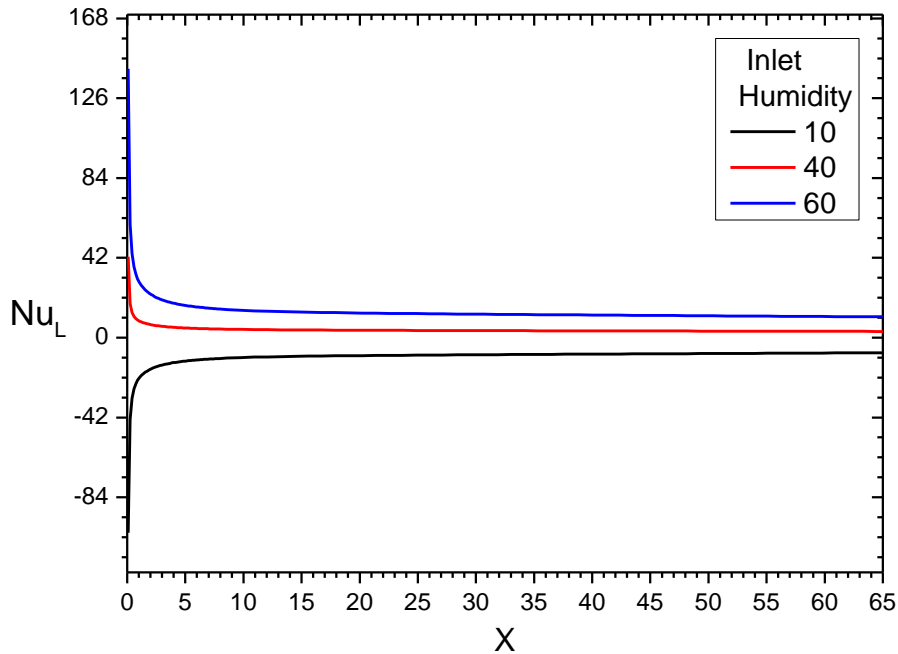|	Tin (°C)	φ_{in} (%)	W_{in} (g/kg)	T_w (°C)	W_w (g/kg)
Case I	40	10	4.598	20	14.9
Case II	40	40	18.547	20	14.9
Case III	40	60	27.979	20	14.9

Figure IV.9: Axial evolution of the latent Nusselt number for different values of inlet humidity

Figure (IV.10) shows the axial evolution of Nu_s for different aspect ratios, $\gamma_1 = 1/130$, $\gamma_2 = 2 \gamma_1$ and $\gamma_3 = 4 \gamma_1$. It is noted that sensible Nusselt number increases with the rise of the aspect ratio. Then, it converges to an asymptotic value for all the aspect ratios ($Nu_s = 4.86$), so, it is concluded that the asymptotic value does not depend on the aspect ratio. As it is mentioned above, this asymptotic value (4.86) corresponds to that of a fully developed value for forced convection [Shah and London [37]; Bejan [38]].
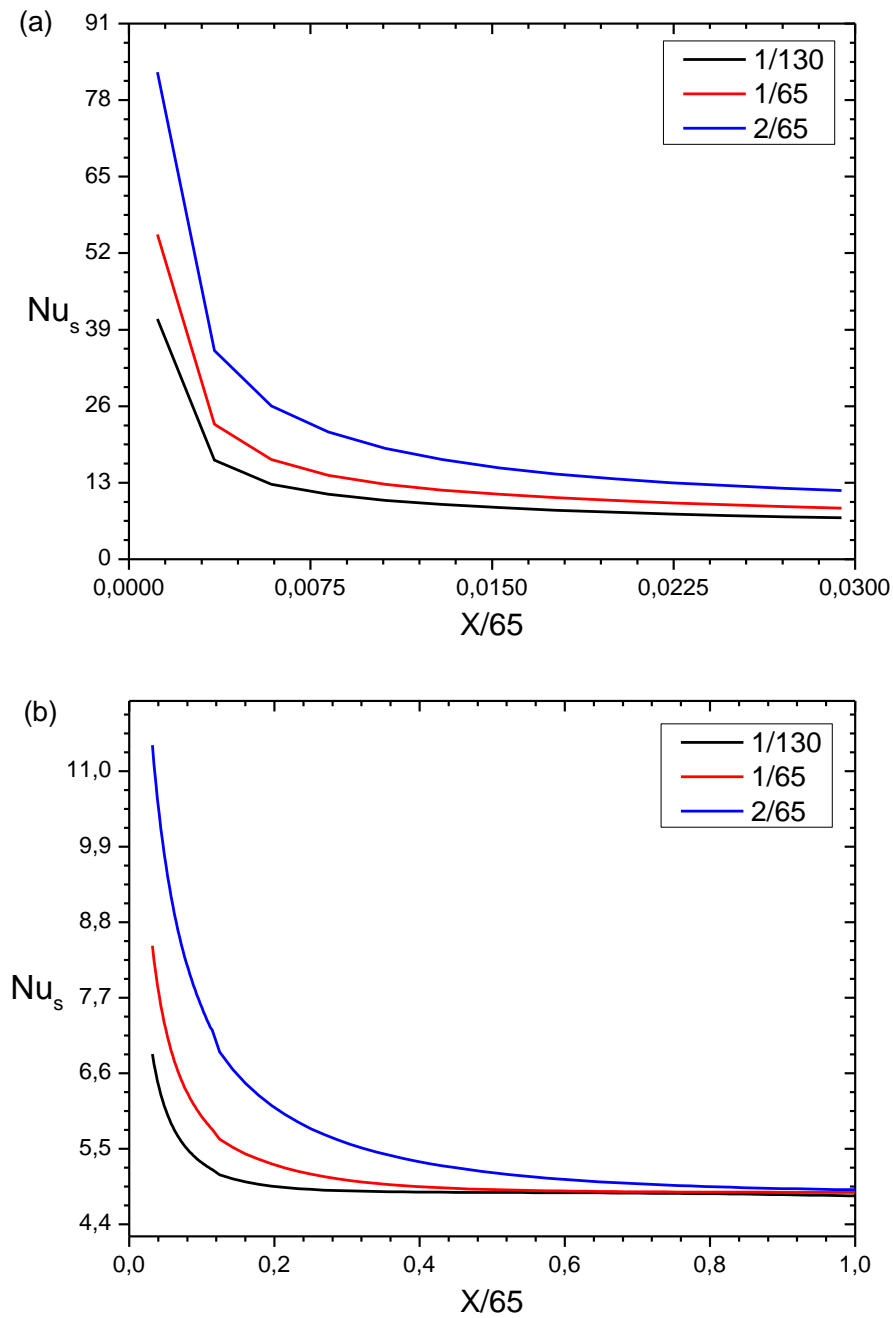
Figure IV.10: Axial evolution of the sensible Nusselt number for different aspect ratios. (a)at the inlet vicinity (b)rest of the channel.

The axial evolution of Nu_s for different values of Reynolds number is shown in figure (IV.11). We note that Nu_s rises with the increase of Re. Knowing that higher Re represents a faster moving vapor-gas mixture, so, faster moving increases the sensible heat transfer from the humid air to the isothermal wall. The sensible Nusselt number paths for different Re converge at the channel outlet.
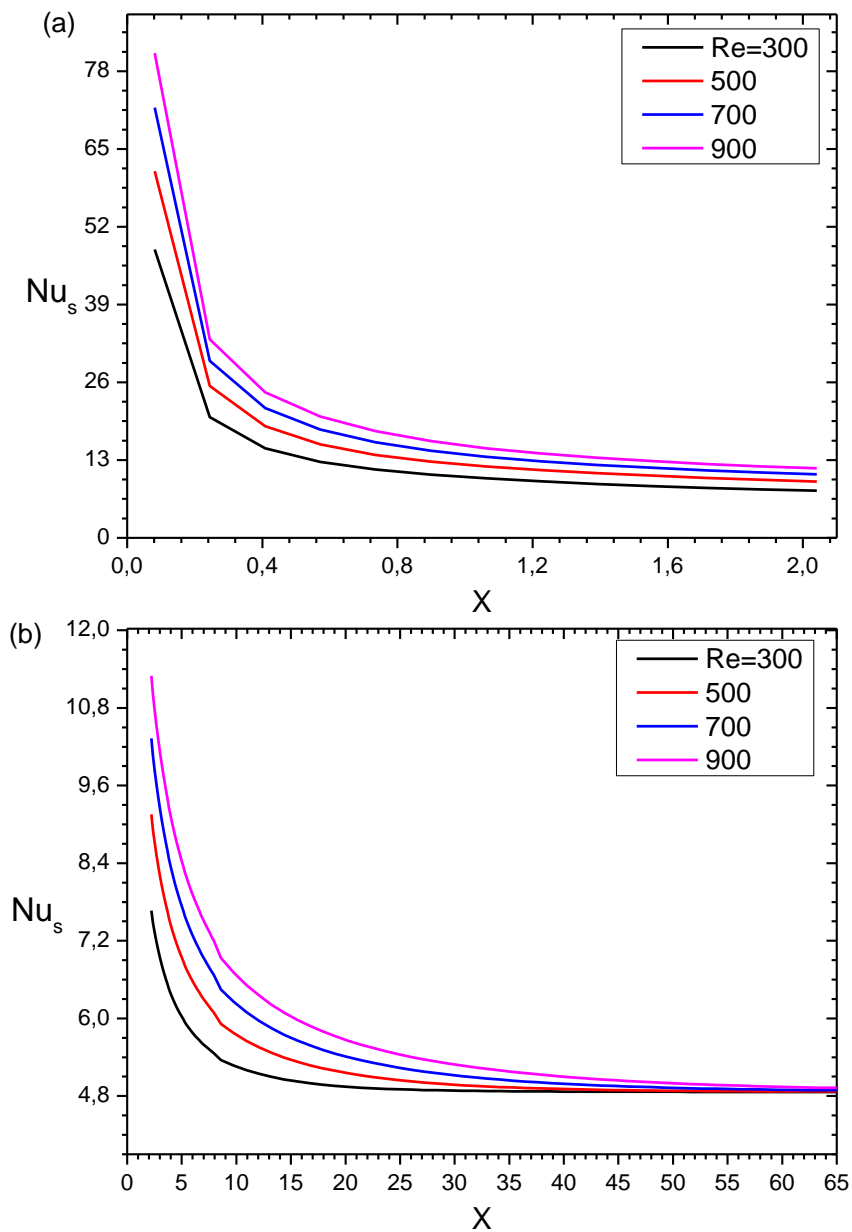
Figure IV.11: Axial evolution of the sensible Nusselt number for different values of Re. (a) at the inlet vicinity (b)rest of the channel.

The axial evolution of latent Nusselt number for different values of Reynolds number is depicted in figure (IV.12). From the comparison of Nu_L for these values of Re, it can be seen that higher inlet velocity promotes latent heat transfer. We note that the latent Nusselt number does not converge to the same value at the outlet for different values of Re, which is the case for sensible Nusselt number.

Figure (IV.13) shows the axial evolution of Latent Nusselt number for different values of aspect ratio, $\gamma_1 = 1/130$, $\gamma_2 = 2\gamma_1$ and $\gamma_3 = 4\gamma_1$. Similarly as Nu_s; at a given position

X, Nu$_L$ increases with the increase of the aspect ratio. This is explained by the rise of the hydraulic diameter.
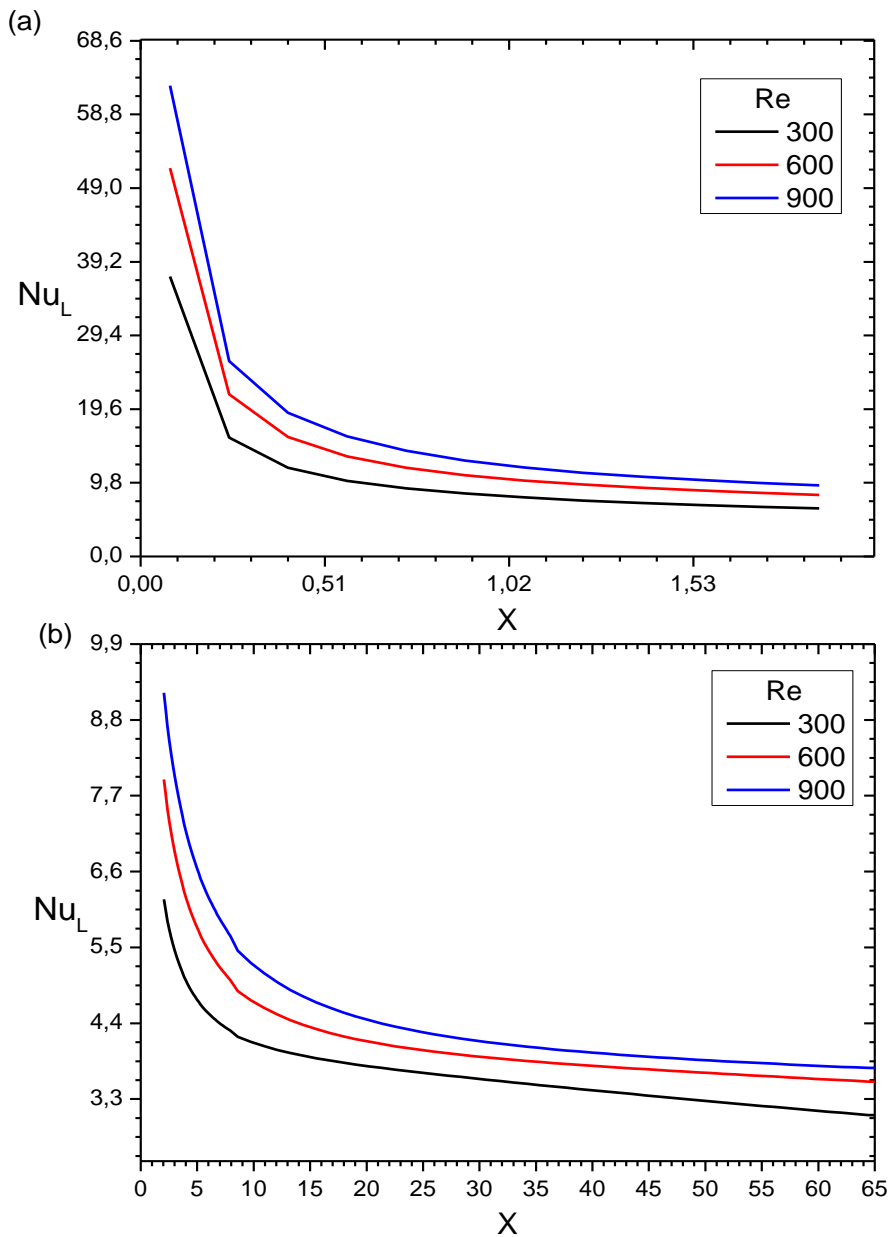
(a)

(b)

Figure IV.12 : Axial evolution of the Latent Nusselt number for different values of Reynolds number. (a) at the inlet vicinity (b)rest of the channel.
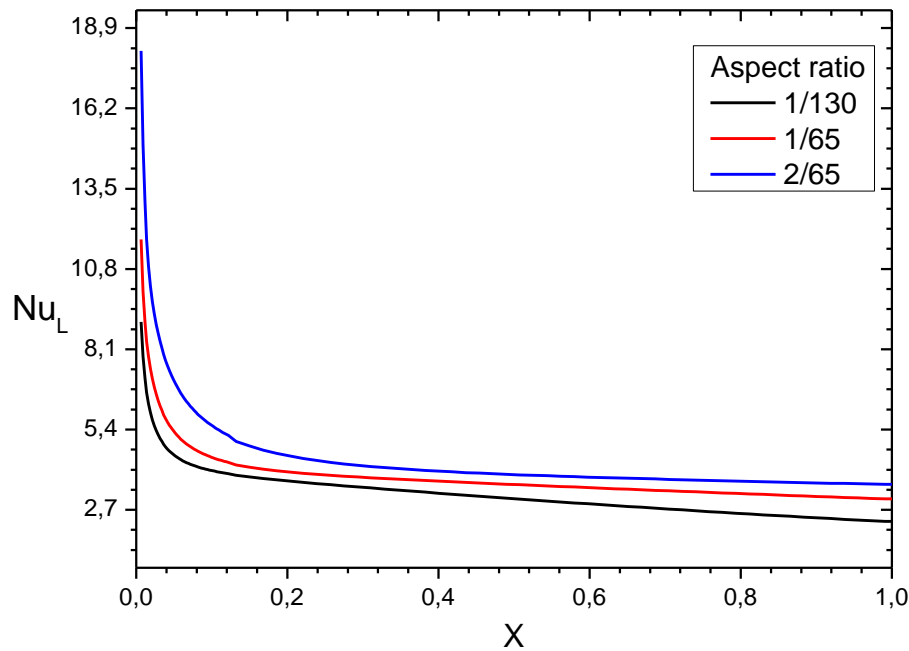
Figure IV.13: Axial evolution of the Latent Nusselt number for different values of aspect ratio

Sherwood number characterizes the mass transfer between the liquid film on the isothermal wall and the flowing mixture. Its axial evolution near the isothermal wall is presented in figure (IV.14).

A global Analysis of this figure shows that the evolution of Sh is monotonous for the case of forced convection. In fact, at the channel inlet, Sh takes high values because of an important concentration gradient, then decreases until it achieves a asymptotic value. It is clear that Sh presents the same trend as Nu_s. This tendency shows clearly the existence of the heat transfer-mass transfer analogy. Moreover, it is important to note that Sh converges to an asymptotic value (4.86), which corresponds to a fully developed flow for forced convection [Bejan [38]]. The aforementioned figure also shows the axial evolution of Sherwood number for different values of Reynolds number. It can be seen that Sherwood number rises with the increase of Re. Since Sh characterizes the mass transfer, it can be stated that higher inlet velocity raises the mass transfer from the humid air to the liquid film. Furthermore, at the channel inlet, Sherwood number converges to the same value for the presented Reynolds numbers.

Figure (IV.15) shows the axial evolution of Sh for different values of aspect ratio, γ_1= 1/130, γ_2= 2 γ_1 and γ_3= 4 γ_1. At a given position X, Sh rises with the increase of the

aspect ratio. Then it converges to asymptotic values: 4.75, 4.86 and 4.88 respectively. These asymptotic values are close to those of a fully developed flow for forced convection [Shah and London [37]]. In our case, we note that the sensible Nusselt number is similar to Sherwood number; this is because Lewis number is close to 1.
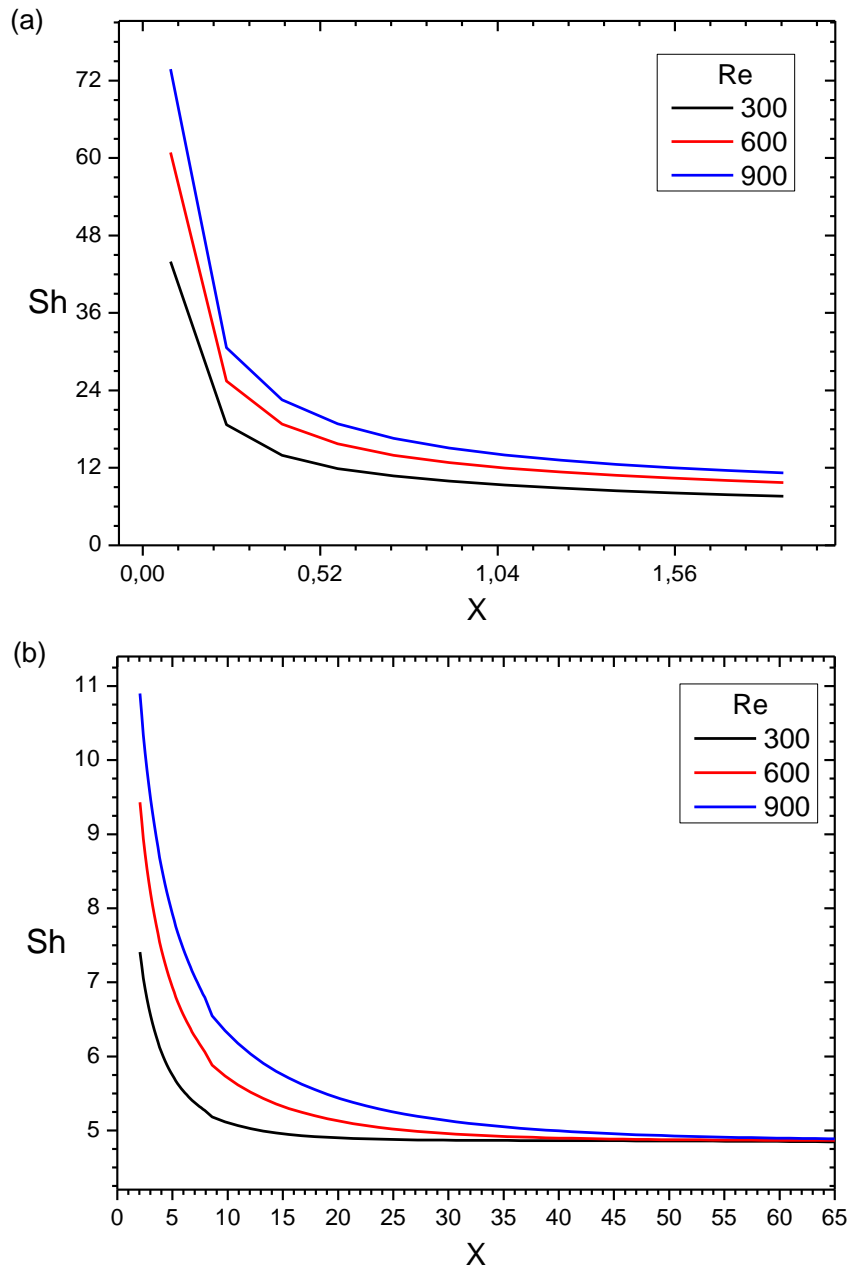
Figure IV.14: Axial evolution of Sherwood number for different values of Reynolds number. (a)at the inlet vicinity (b)rest of the channel.
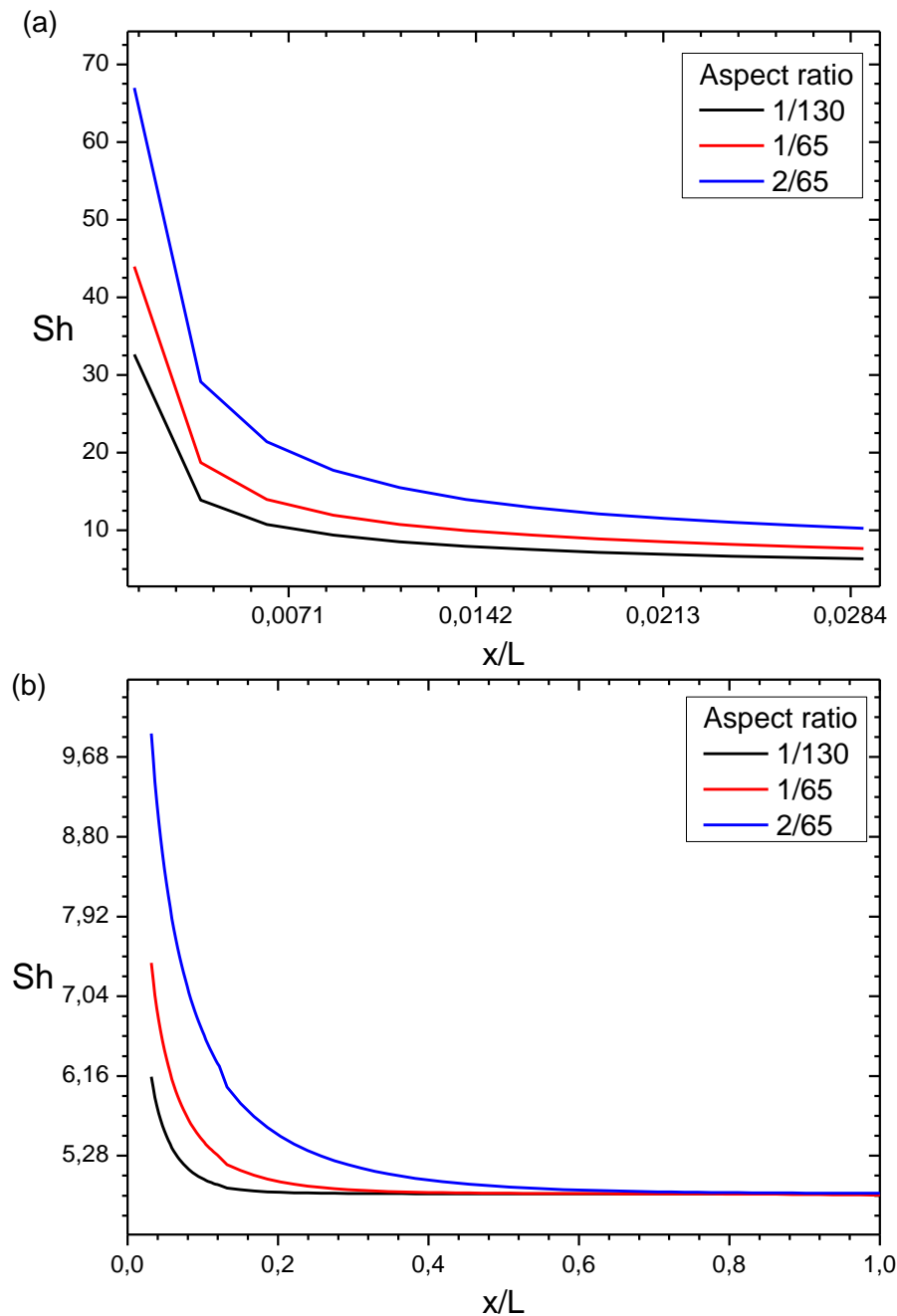
Figure IV.15: Axial evolution of Sherwood number for different values of aspect ratio. (a)at the inlet vicinity (b)rest of the channel.

IV.5   The effect of inlet parameters on the condensed mass flow rate

IV.5.1   Effect of inlet relative humidity on the condensed mass flow rate

To study the influence of the inlet relative humidity on the mass flow rate, we present the numerical simulation results for different values of air inlet relative humidity. The studied channel (Figure II.1) is formed of two vertical plates with an aspect ratio of $\gamma =$

1/65). The presented curves are shown for an imposed temperature on the wet wall T_w=20°C (W_w =14.9g/kg) while the other plate is adiabatic and dry. Ambient air is characterized by an inlet temperature T_{in}=40°C and a variable relative humidity. The air velocity at the channel inlet is u_o= 0.0025 m/s (Re=400).

Figure (IV.16) illustrates the total mass flow rate as function of inlet relative humidity. The curve is based on a wide range of φ_{in} (From 10% to 100 %) which corresponds to a range of W_{in} between 4.589 g/kg and 47.165 g/kg.

As we are going to see in the next section, since the axial evolution of the mass flow rate has positive values for a relative humidity lower than 30%, the total mass flow rate has positive values as well, which is the evaporation case. This occurs because in this range of inlet relative humidity, the concentration at the channel inlet is lower than that of the wall. However, for relative humidity above 30%, the total mass flow rate is negative which corresponds to condensation, where the concentration at the inlet becomes higher than that of the wall. The absolute value of the total mass flow rate increases with φ_{in}, implying that the condensed flow rate becomes more intense when the inlet relative humidity increases (the inlet concentration increases as well). We notice that the total mass flow rate has linear relationship with inlet relative humidity, where the gradient is constant.
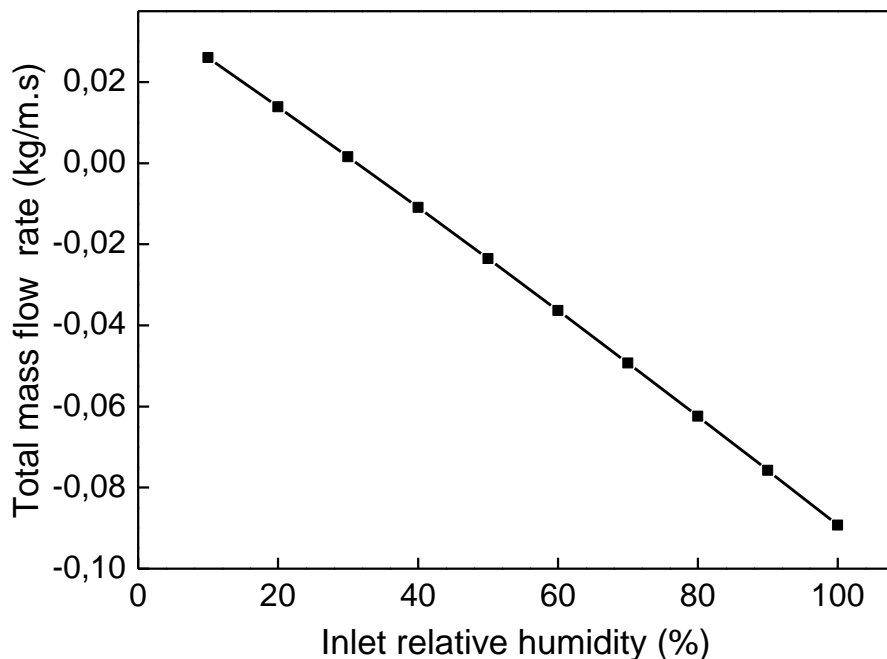

Figure IV.16: Total mass flow rate vs. inlet relative humidity

The axial evolution of the mass flow rate of the condensed vapor is presented in figures (IV.17). We note positive values of mass flow rate for φ_{in} = 10 %, these positive values

indicate flow towards the adiabatic wall. It follows that in this case, water is evaporated from the film and transferred to the mixture flow. It is noticed, moreover, that for φ_{in} = 10 % (W_{in} = 4.598 g/kg) the air mass fraction is lower than the one of the film (W_w= 14.9 g/kg). This is explained by the evaporation case. When φ_{in} = 30%, the values of the mass flow rate approach zero indicating that the phase change and interfacial mass transfer are negligible for this case, where the concentration at the inlet and that of the wall are close (W_{in}= 14.467 g/kg).

On the other hand, the other cases (φ_{in} =40 and up), where the air mass fraction is greater than that of the film, the water vapor contained in air condenses on the wet wall. This condensation becomes   increasingly intense as φ_{in} increases. This is due to the rise of the difference between the inlet vapor mass fraction and that of the wall.

For the case of φ_{in} =10%, the mass flow rate decreases and takes positive values tending to zero at the channel outlet. These positive values corresponds to the film evaporation case because the air mass fraction at the channel inlet is below than that of isothermal wall. This decrease along the channel is due to the increase of the average concentration (see figure (of Wm) for φ_{in} =10%) which leads to lower phase change when the mixture advances through the channel.

 For the other cases, φ_{in} = 40% and 80%, we observe that the absolute value of mass flow rate increases with φ_{in}. It should be known that the increase of the relative humidity means the increase of water vapor concentration. In the other case, the decrease of the relative humidity leads to an increase of the air concentration, which represents a resistance to heat and mass transfer, causing resistance to the condensed flow rate. So the reduction of the condensed mass flow rate is explained by the resistance caused by the presence of the noncondensable gas which is the air in our case.

(a)

(b)
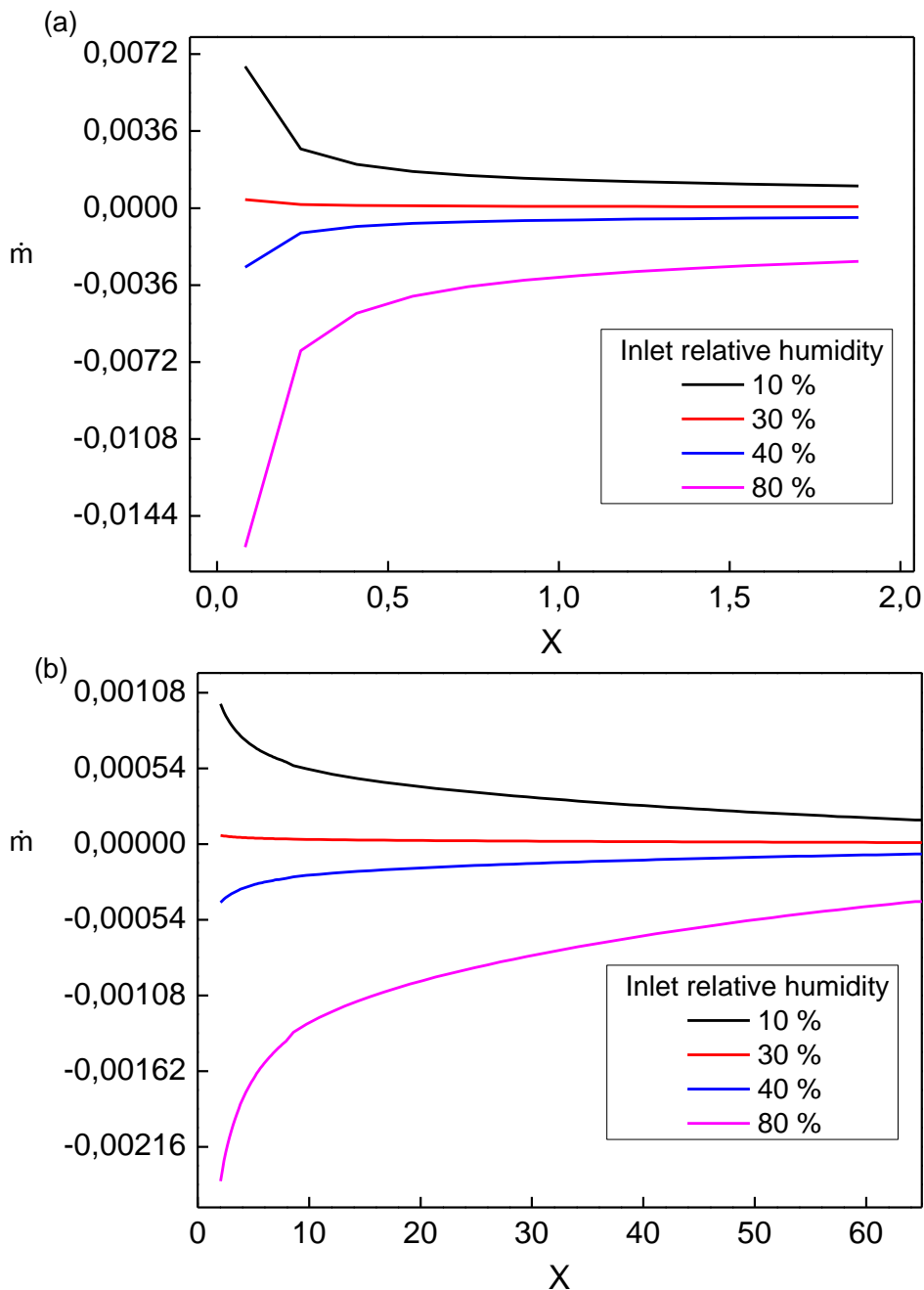
Figure IV.17: Axial evolution of the mass flow rate for different values of inlet relative humidity. (a) at the inlet vicinity (b)rest of the channel.

IV.5.2 Effect of inlet temperature on the condensed mass flow rate

A comparison of results for a range of inlet temperatures (T_{in}) was made while fixing the other parameters, Tw = 20 °C, φ_{in} = 40% and Re = 300, γ = 1/65.

Figure (IV.18) depicts the total mass flow rate as function of the inlet temperature for a fixed wall temperature. For an inlet temperature of T_{in} lower than 35 °C, the total mass flow rate has a positive value which is the evaporation case, indicating flow towards the right wall of the channel. It means that water is evaporated from the liquid film. Moreover, it should be noticed that, in this case, the film is evaporated even when

the inlet temperature is greater than the wall temperature; this is due to the concentration, where the inlet concentration is lower than the wall concentration. For the inlet temperatures greater than 35 °C, condensation occurs. The total mass flow rate rises with the increase of the inlet temperature. The relationship between the total mass flow rate and the inlet temperature is not linear, which is not the case for the inlet relative humidity (see figure IV.16), where we note a decrease of the gradient. This means that a small increase in the inlet temperature leads to a higher rise of condensed mass flow rate.
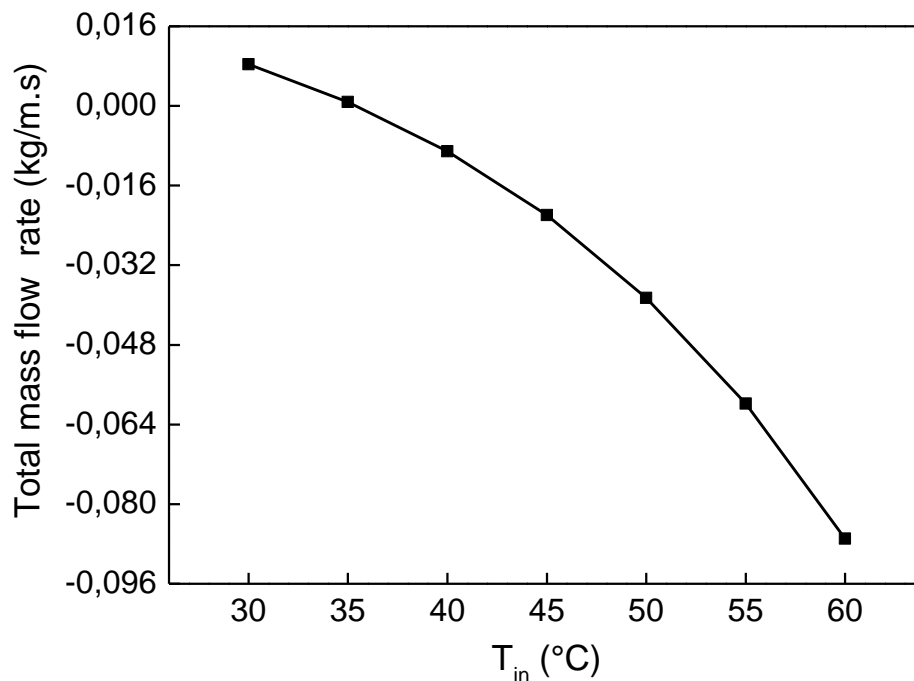
Figure IV.18: Total mass flow rate vs. T_{in}

Figure (IV.19) shows the axial evolution of mass flow rate for different values of the inlet temperature. This figure is based on a range of inlet temperatures between 30 °C and 60 °C. For the case of T_{in} = 30°C, we note a positive value of the mass flow rate which indicates flow towards the right wall of the channel. As it is explained in the last paragraph, this is because the wall concentration is higher than the inlet concentration. However, for inlet temperatures higher than 40 °C, the mass flow rate has negative values, which is the condensation case.

Moreover, it should be noticed that in this case, the film is evaporated even when the inlet temperature is greater than the wall temperature; this is due to the concentration, where the inlet concentration is lower than the wall concentration. For the inlet temperatures equal or greater than 40°C, condensation occurs. We notice that at given position X, an increase of the inlet temperature leads to an increase of the mass flow

rate for a fixed wall temperature (an increase in the absolute value of the mass flow rate) owing to the increase of the ΔT. It is noted that in the inlet vicinity, high amounts of mass flow rate, this is relatively due to a high difference of temperature and concentration between the inlet and the wall, compared to the rest of the channel. It should be mentioned that the increase in the mass flow rate due to the increase of inlet temperature is contributed by the increase of the inlet concentration as well, because the rise in inlet temperature leads to a rise in inlet concentration for a given relative humidity.
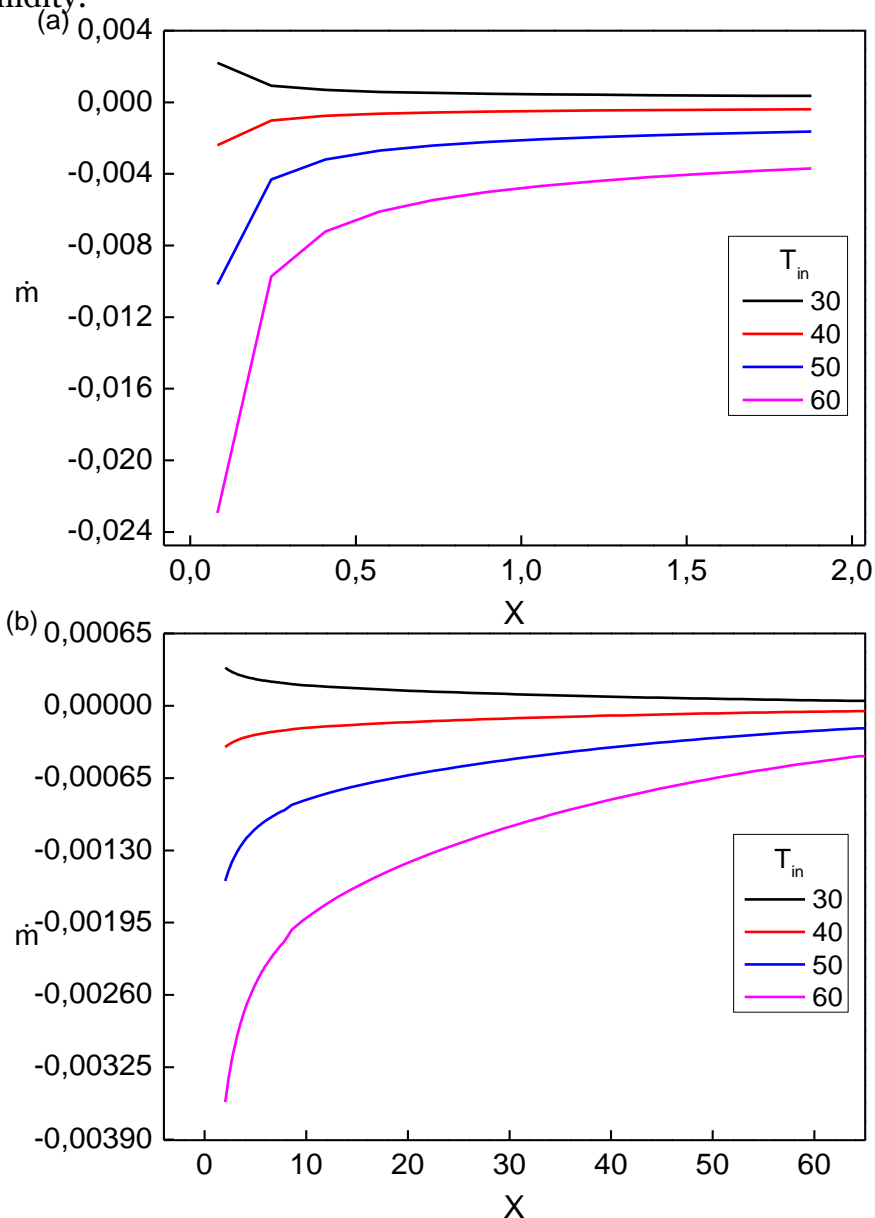

Figure IV.19: Axial evolution of mass flow rate for different values of inlet temperature. (a) at the inlet vicinity (b)rest of the channel.

IV.5.3 Effect of inlet Reynolds number on the condensed mass flow rate

In this part, we present a numerical study about the effect of Reynolds number on the mass flow rate. The results presented here are calculated with:

$$Tw = 20\ ^{\circ}C,\ Tin = 40\ ^{\circ}C,\ \varphi_{in} = 40\ \%,\ \gamma = 1/65.$$

Figure (IV.20) illustrates the total mass flow rate as function of the inlet Reynolds number. It is based on a range of Reynolds numbers between 200 and 1000, which corresponds to an inlet velocity range between (0.109 m/s et 0.544 m/s). The study has been carried out for range values of Reynolds numbers with a constant inlet relative humidity and inlet temperature in order to be able to visualize the effect of Reynolds number on the mass flow rate. We note that the absolute value of mass flow rate increases monotonously with Reynolds number, which implies the rise of the condensed mass flow rate with the increase of inlet velocity. So, the faster the flow, the more condensed mass flow rate. The rise of the condensed mass flow rate as function of Reynolds number is explained by the rise of latent heat transfer, because as we have seen above, (see figure IV.63), the latent Nusselt number increases with the rise of Reynolds number.
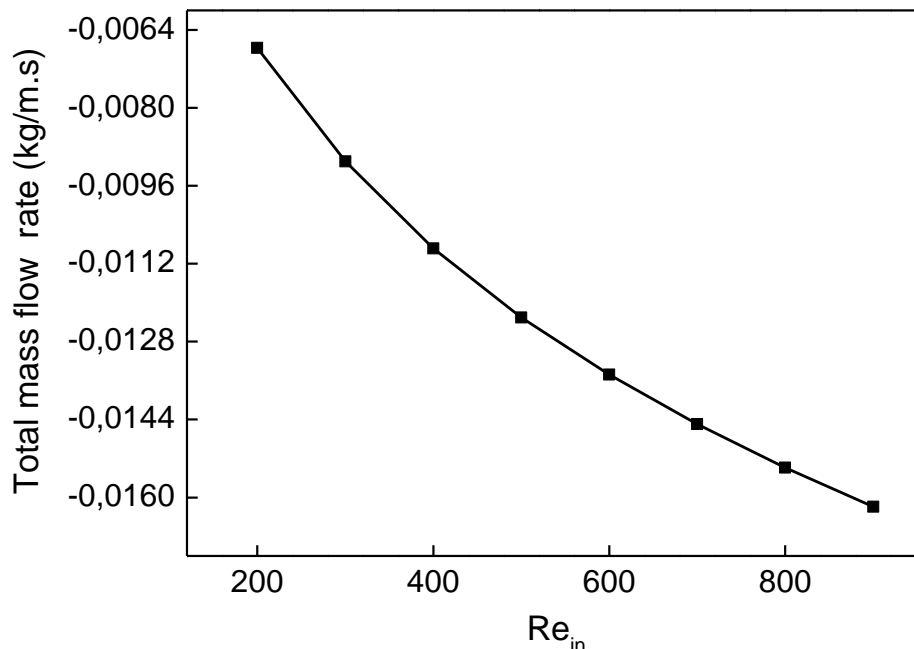
Figure IV.20: total mass flow rate vs. Inlet Reynolds number

We note that the gradient is decreasing, which means that the mass flow rate will stay constant after a critical value of Reynolds number. This critical value is not achieved in this study due to the limitation of the used assumptions (see the third assumption). Figure (IV.21) shows the axial evolution of mass flow rate on the isothermal wall, for

different values of Reynolds number with constant inlet relative humidity and inlet temperature. It should be noted that at a given axial position, the condensed mass flow rate increases as the Reynolds number increases, and that it tends uniformly to an asymptotic value close to zero as X increases. This asymptotic behavior is obviously due to the fact that the temperature and absolute humidity of the air approach the corresponding wall values as X increases. This is because the gaps of temperature and concentration are the generator of heat and mass transfer. When it gets narrower, the heat and mass transfer decrease considerably.

Figure IV.21: Axial evolution of mass flow rate for different values of inlet Reynolds number. (a)at the inlet vicinity (b)rest of the channel.

IV.5.4 Effect of aspect ratio on the condensed mass flow rate
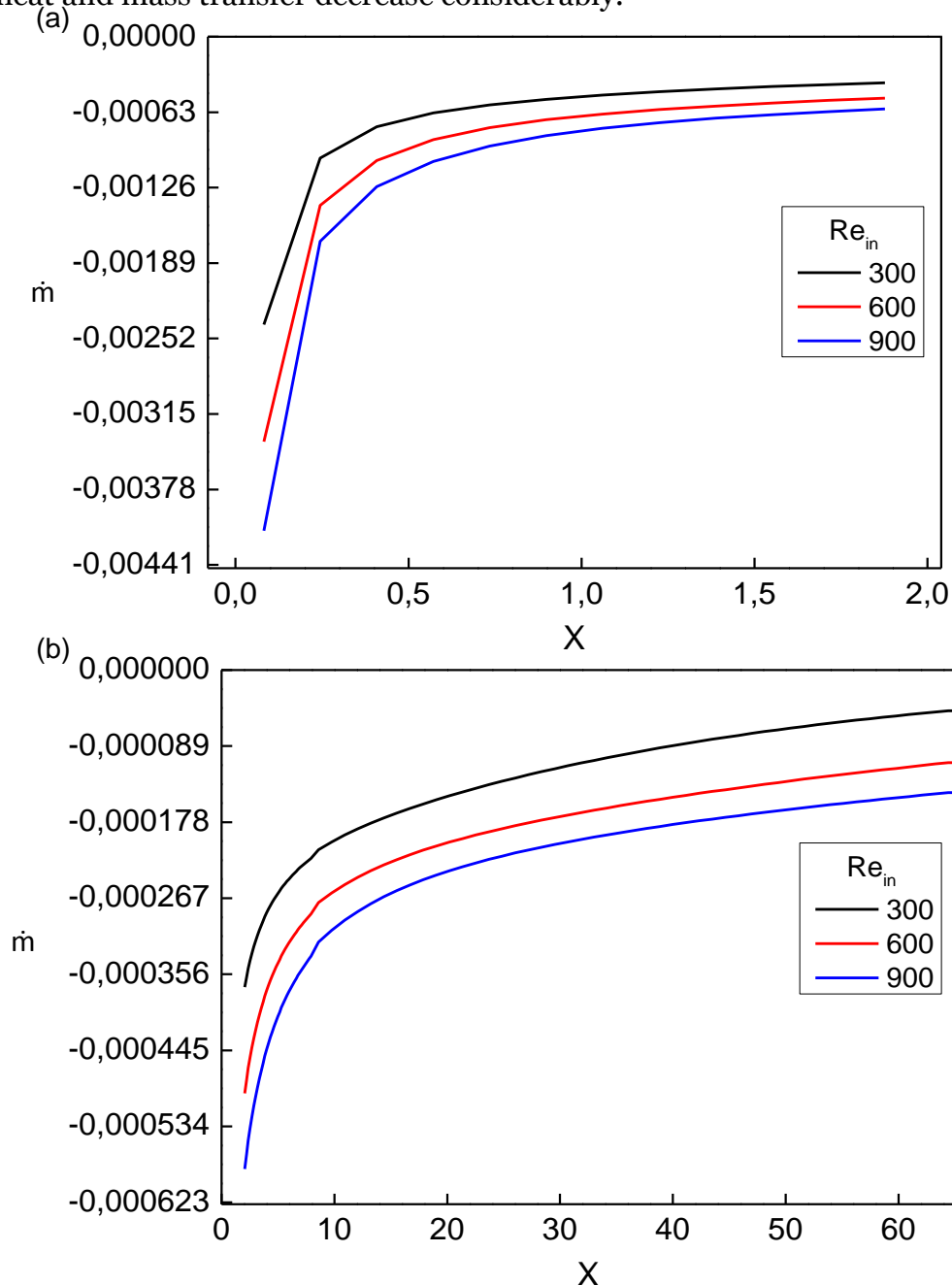
In this section, the effect of aspect ratio will be presented. We have varied the aspect ratio of the channel as it happens by pulling aside between the two plates, for four different cases $\gamma_1 = 1/130$, $\gamma_2 = 2\gamma_1$, $\gamma_3 = 4\gamma_1$ and $\gamma_4 = 8\gamma_1$ in order to be able to examine its effect on the condensed mass flow rate.

Figure (IV.22) depicts the axial evolution of the condensed mass flow rate as function of different values of the aspect ratio. It is noted that for all cases, condensation occurs. The liquid film temperature is maintained constant at $T_w = 20$ °C ($W_w = 14.9$ g/kg) where that of the channel inlet is $T_{in} = 40$°C; $\varphi_{in} = 40\%$ ($W_{in} = 18.547$ g/kg). Prandtl number is Pr = 0.71 and that of Schmidt is Sc=0.598. Reynolds number is 300 and the air inlet velocity varies with the pulling aside of the plates due the interdependence between the velocity and the hydraulic diameter on the Reynolds number expression. For the being considered aspect ratios, it should be noticed that at a given position x, the mass flow rate rises with the increase of the aspect ratio, this is due to the increase of the hydraulic diameter; then it tends uniformly to an asymptotic value close to zero as X increases. This asymptotic behavior is obviously due to the fact that the temperature and absolute humidity of the air approach the corresponding wall values as X increases, because the thermal and concentration driving forces are the generator of heat and mass transfer, and when they get smaller, the heat and mass transfer decrease considerably. So, we can conclude that the influence of the aspect ratio on the axial mass flow rate decreases along the tube.
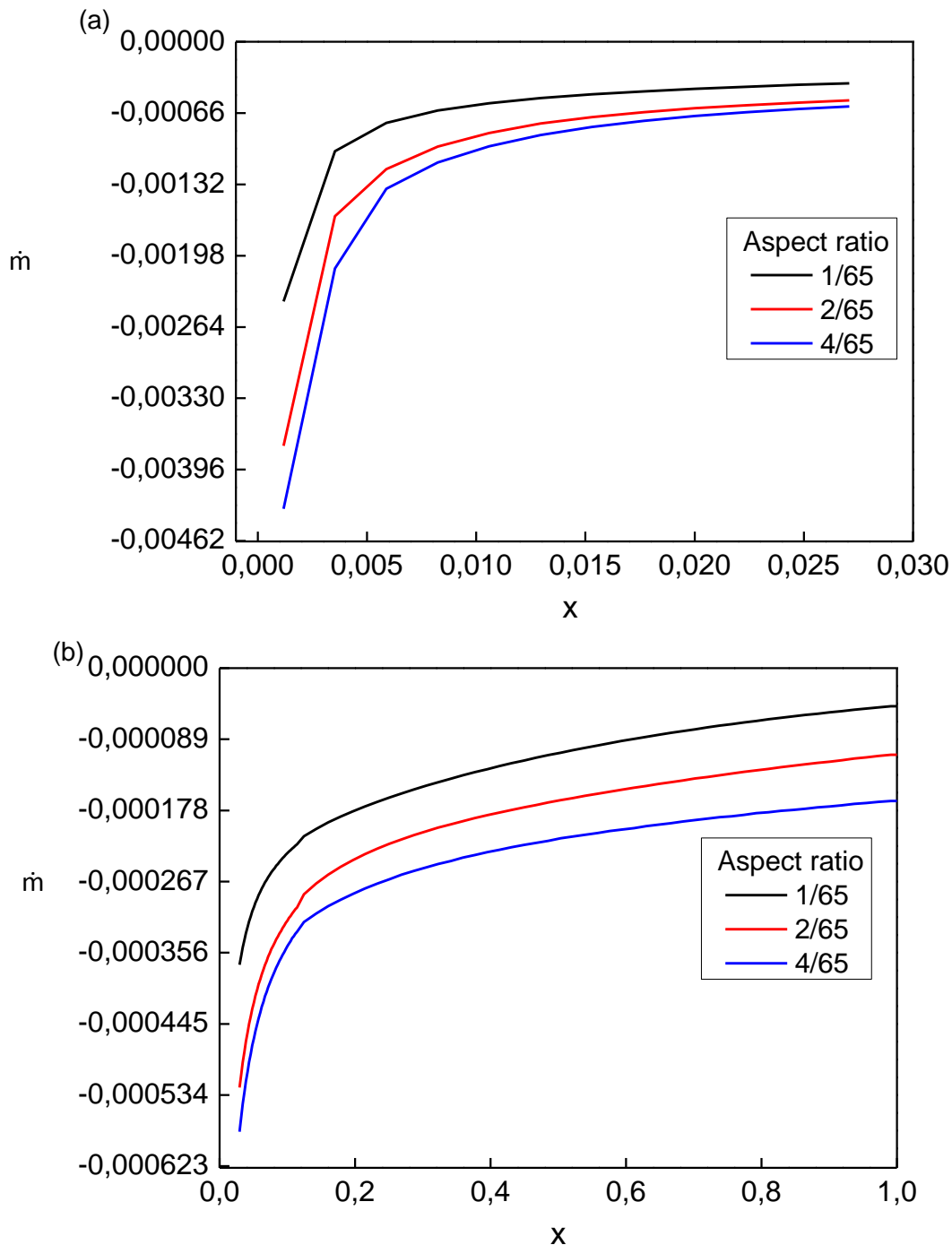
Figure IV.22: Axial evolution of mass flow rate for different values of aspect ratio. (a)at the inlet vicinity (b)rest of the channel.

IV.6   Conclusion

In this chapter, we have presented the results of the numerical simulation of a parametric study of coupled transfers of heat and mass with phase change in a vertical channel. The results show that the increase of inlet parameters T_{in}, φ_{in} and Re_{in} as well as the aspect ratio promotes the condensed flow rate. It has been found that the condensed flow rate decreases monotonously along the channel. At a given axial

position the mass flow rate increases with the rise of the aforementioned parameters. These parameters have the same impact on the released heat. It has been shown that latent heat is more important than the sensible heat. It has been found that the sensible heat and the mass transfer are promoted by the increase of the aspect ratio and the Reynolds number.

Chapter V

GENERAL CONCLUSION AND PERSPECTIVE

The presented work in this thesis is a numerical study for forced convection with condensation in a vertical channel. This is formed of two parallel plates; one of them is maintained at a uniform and constant temperature where the other is adiabatic and dry. A flow of vapor in presence of a noncondensable gas goes down through the channel. The isothermal wall is covered by a thin film due to condensation. The mathematical modeling of this physical problem is based on conservation equation of: continuity, momentum, energy and chemical species. The thermophysical properties are considered constant and the Boussinesq approximation has been adopted. Simplifying assumptions have been introduced and justified. The resulting simplified equations system, which takes into account the axial diffusion, is solved numerically using finite volume method. The coupling velocity-pressure is treated by SIMPLER algorithm. A computation code has been developed and validated with a previous published work available in the literature. A wide range of inlet input parameters for the mixture of steam-air has been used to study the heat and mass transfer for condensation case, where the condensed mass flow rate has been evaluated for different values of inlet parameters such us T_{in}, φ_{in} and Re_{in}.

The main results drawn from this work can be summarized as follow:

- The increase of the inlet humidity of the mixture promotes the condensation of the water vapor contained in the air and increases the latent heat transfer between the liquid film and the humid airflow.

- A decrease of the inlet humidity of the mixture promotes the evaporation of the liquid film even the inlet temperature is higher than the wall's.
- The presence of the noncondensable gas reduces condensation and heat transfer.
- The condensed rate increases with the mixture inlet velocity to a certain stage where it remains constant. At this stage, the increase of inlet velocity has no effect on the condensed mass flow rate.
- The increase of the inlet temperature raises the condensed mass flow rate.
- The rise of the aspect ratio for a fixed Reynolds number promotes the condensed flow rate.
- The heat transfer by latent heat is more important than the sensible heat.
- The sensible heat and mass transfer is accelerated when the flow is fast, this is by either increasing the velocity or the aspect ratio.
- The adiabatic wall is cooled by a momentum transfer and its concentration is decreased due a momentum transfer as well.

The perspectives of development of this work can be:

- Adaptation of a more complete model that takes into account the variability of the thermophysical properties as a function of temperature and concentration.
- The analysis can be extended to laminar film condensation at both plates inside a vertical channel. This can be done easily by treating the right plate of the present model as a symmetry line.
- Taking into account the liquid film thickness.

Appendix A

Temperature and mass fraction of the mixture

The mixture temperature that we are going to talk about is based on that of the flow rate. Indeed, considering a flat section S_0 in an internal flow. This section is bounded and its contour composed of tube wall (Usually, S_0 is perpendicular to the axial direction of the flow; it is referred to "cross section").

Reminding the definition of the volume flow rate Q_v and the mass flow rate Q_m through the cross section S_0 :

$$Q_v = \int_{S_0} \vec{v}.\vec{n}ds \tag{A.1}$$

$$Q_m = \int_{S_0} \rho\vec{v}.\vec{n}ds \tag{A.2}$$

We denote by V_m (average velocity or mixture velocity) the uniformly distributed velocity which ensures the same flow rate through the section S_0.

$$Q_v = S_0 V_m \qquad \leftrightarrow \qquad V_m = \frac{1}{S_0}\int_{S_0} \vec{v}.\vec{n}ds \tag{A.3}$$

This average velocity is simply denoted by V when there is no notation ambiguity. In the same manner as (A.2), we define the thermal rate. It is defined as the transferred energy by the fluid through a section S_0.

$$Q_e = \int_{S_0} \rho C_p T \vec{v}.\vec{n}ds \tag{A.4}$$

The concept of "mixture temperature" is of the same origin as that of the mixture velocity. It characterizes the temperature T_m of an isothermal flow which carries the same thermal rate with the same volume flow rate. We put:

$$Q_e = \int_{S_0} \rho C_p T \, \vec{v} . \vec{n} ds \tag{A.5}$$

Hence

$$T_m = \frac{Q_e}{\int_{S_0} \rho C_p \vec{v} . \vec{n} ds} \tag{A.6}$$

If the section S_0 is a cross section of the flow in a channel, then the normal $\vec{n}$ is parallel to the x direction of the flow. The expression of T_m becomes:

$$T_m = \frac{\int_0^{2b} \rho v T dy}{\int_0^{2b} \rho v dy} \tag{A.7}$$

Because of the similarity between the heat and mass convection, we deduce the concept of average mass fraction by:

$$C_m = \frac{\int_0^{2b} \rho v C dy}{\int_0^{2b} \rho v dy} \tag{A.8}$$

It is important to note that, T_m, is referred to ''average temperature'' in equation (A.7) show the velocity weighted average.

Appendix B

$\mathbf{P}_{\textbf{sychrometrics}}$

In the problems of air conditioning, the humid air can be considered as an ideal mixture of two ideal gases: the dry air and the vapor water, Bruhhat [39]. This mixture is characterized, beside thermodynamic properties, by the psychometric properties. We define some properties which are in relation with our problem, Bailly [40].

a. Water vapor concentration (W)

It is the ration between the mass of water vapor m_v and the mass of the dry air m_a contained in a same volume of humid air:

$$C = \frac{m_v}{m_a} \tag{B.1}$$

Considering that the water vapor-air mixture is a mixture of ideal gases, the relation (B.1) is written:

$$C = \frac{M_a}{M_v} \frac{1}{\dfrac{P}{\varphi_{in}\, P_{sat}} - 1} \tag{B.2}$$

Where φ_{in} is the relative humidity, P_{sat} is the water vapor pressure at the saturation, P is the total pressure of water vapor-air mixture. M_a and M_v are the molecular weights of air and water vapor respectively.

b. Relative humidity φ_{in}

It is defined as the ratio between the real fraction of water and that at the saturation:

$$\phi = \frac{m_v}{m_{vsat}} \tag{B.3}$$

Applying the ideal gas law, we can write it as follows:

$$\phi = \frac{P_v}{P_{vsat}} \tag{B.4}$$

c. Pressure at the saturation

It is the vapor pressure at which the considered humid air cannot absorb any additional amount of water vapor. Its value can be estimated from the flowing relation, Vashon [41] and Debbissi et al. [42].

$$\log_{10} p_{sat}(T) = 28.590151 - 8.2 \log_{10} T + 2.4804 \times 10^{-3}T - \frac{3142.32}{T} \qquad (\mathbf{B.5})$$

Where the pressure is expressed in bar and the temperature is expressed in Kelvin.

d. Concentration at the saturation

It is the fraction of water at the saturation state of the considered air. We assume that the water vapor-air mixture is an ideal mixture, we can write, Debbissi et al. [42]et Bailly [40]:

$$C_{sat} = \frac{\dfrac{M_a}{M_v}}{\dfrac{P}{P_{sat}} + \dfrac{M_a}{M_v} + 1} \qquad (\mathbf{B.6})$$

Appendix C

Thermophysical properties

The properties of air, water vapor, mixture and liquid film adopted in this work are calculated by the following relations taken from Fujii et al. [43]:

Air

Dynamic viscosity

$$\mu_a = \frac{1.488 \times 10^{-3} T^{1.5}}{118 + T} \qquad \text{(kg/ms)} \qquad (\mathbf{C.1})$$

Thermal conductivity

$$k_a = \frac{1.195 \times 10^{-3} T^{1.6}}{118 + T} \qquad \text{(W/mK)} \qquad (\mathbf{C.2})$$

Specific heat

$$Cp_a = (1 + 2.5 \times 10^{-3} T^3) \times 10^3 \qquad \text{(J/kg K)} \qquad (\mathbf{C.3})$$

Vapor

Dynamic viscosity

$$\mu_v = [8.02 + 0.04 \times (T - 273.16)] \times 10^{-6} \qquad \text{(kg/ms)} \qquad (\mathbf{C.4})$$

Thermal conductivity

$$k_v = \left[1.87 + 1.65 \times 10^{-3}(T - 273.16)^{\frac{9}{7}} + 5.7 \times 10^{-13}(T - 273.16)^{5.1}\right] \times 10^{-2} \quad \text{(W/mK)} \quad (\mathbf{C.5})$$

Specific heat

$$Cp_a = [1.863 \times 10^3 + 1.65 \times 10^{-3}(T - 273.16)^{2.5} + 1.2 \times 10^{-18}(T - 273.16)^{8.5}] \times 10^{-2} \quad \text{(J/kgK)} \qquad (\mathbf{C.6})$$

Mixture(Air+ Water vapor)

Density

$$\rho = \frac{2.167 \times 10^{-2}}{1 - (1 - 0.622)C_a}\left(\frac{P}{T}\right) \qquad (kg/m^3) \qquad (C.7)$$

Dynamic viscosity

$$\mu = \frac{\mu_a}{1 + \left(\frac{x_v}{x_a}\right)\phi_{av}} + \frac{\mu_v}{1 + \left(\frac{x_a}{x_v}\right)\phi_{va}} \qquad (kg/ms) \qquad (C.8)$$

$$\phi_{ij} = \frac{\left\{1 + \left(\frac{\mu_i}{\mu_j}\right)^{\frac{1}{2}}\left(\frac{M_i}{M_j}\right)^{\frac{1}{4}}\right\}^2}{\frac{4}{\sqrt{2}}\left(1 + \frac{M_i}{M_j}\right)^{\frac{1}{2}}} \quad i,j = a, v \qquad (C.9)$$

Where x_a and x_v are the mole fraction of air and vapor respectively. The molecular weight of the air and the vapor are:

$M_a = 28.96$ (kg/kmol)

$M_v = 18.02$ (kg/kmol)

Thermal conductivity

$$k = \frac{k_a}{1 + \left(\frac{x_v}{x_a}\right)A_{av}} + \frac{k_v}{1 + \left(\frac{x_a}{x_v}\right)A_{va}} \qquad (W/mK) \qquad (C.10)$$

where

$$A_{ij} = \frac{1}{4}\left[1 + \left\{\frac{\mu_i}{\mu_j}\left(\frac{M_i}{M_j}\right)\frac{\left(1 + \frac{S_i}{T}\right)}{\left(1 + \frac{S_j}{T}\right)}\right\}^{\frac{1}{2}}\right]^2 \frac{\left(1 + \frac{S_{ij}}{T}\right)}{\left(1 + \frac{S_j}{T}\right)} \qquad (C.11)$$

With:

$S_a = 115.5$

$S_v = 559.5$

$S_{ij} = 0.733\sqrt{S_i S_j}$

Specific heat

$$Cp = Cp_a C_a + Cp_v(1 - C_a) \qquad \text{(J/kg K)} \qquad (\mathbf{C.12})$$

Mass diffusivity

$$D = 8.07 \times 10^{-10} \times T^{1.833} \qquad \text{(m}^2/\text{s)} \qquad (\mathbf{C.13})$$

Liquid water

Density

$$\rho_L = \frac{10^3}{1 + 8.7 \times 10^{-6}(T - 273.16)^{1.83}} \qquad \text{(kg/m}^3) \qquad (\mathbf{C.14})$$

Dynamic viscosity

$$\mu_L = 2.4 \times 10^{-5} \times 10^{\left(\frac{251}{T-273.16+135}\right)} \qquad \text{(kg/ms)} \qquad (\mathbf{C.15})$$

Thermal conductivity

$$k_L = 0.6881 - 4 \times 10^{-6} \times (408.16 \times T)^{2.1} \qquad \text{(W/mK)} \qquad (\mathbf{C.16})$$

Specific heat

$$Cp_L = 4.179 \times 10^3 + 7.9 \times 10^{-5}(T - 273.16)^{2.9} \qquad \text{(J/kg K)} \qquad (\mathbf{C.17})$$

Latent heat

$$h_{fg} = 2.5016 \times 10^6 + 2.370 \times 10^5(T - 273.16) \qquad \text{(J/kg)} \qquad (\mathbf{C.18})$$

It is important to note that in these equations, the temperature T is expressed in *kelvin* (K) and the pressure P in *bar*.

Bibliography

[1]   W. Nusselt, "The condensation of steam on cooled surfaces," *Zeitschrift des Vereines Deutscher Ingenieure,* vol. 60, no. 27, pp. 541-575, 1916.

[2]   W. Rohsenow, "Heat transfer and temperature distribution in laminar film condensation," *Trans.A.S.M.E,* vol. 78, pp. 1645-1648, 1956.

[3]   E.M. Sparrow, J.L. Gregg, "A Boundary-Layer Treatment of Laminar-Film Condensation," *Journal of Heat Transfer Trans. ASME,* vol. 18, pp. 13-18, 1959.

[4]   J.C. Koh, E.M. Sparrow, J.P. Hartnett, "The Two Phase Boundary Layer in Laminar Film Condensation," *International Journal of Heat and Mass Transfer,* vol. 2, pp. 69-82, 1961.

[5]   Koh, J.C.Y., "Film Condensation in a Forced-Convection Boundary-Layer Flow," *International Journal of Heat and Mass Transfer,* vol. 1980, pp. 161-177, 1962.

[6]   I.G. Shekriladze, V.I. Gomelauri, "Theoretical study of laminar film condensation of flowing vapour," *International Journal of Heat and Mass Transfer,* vol. 9, pp. 581-591, 1966.

[7]   F. Dobran, R. S. Thorsen, "Forced flow laminar filmwise condensation of pure saturated vapor in a vertical tube," *International Journal of Heat and Mass Transfer,* vol. 23, pp. 161-177, 1980.

[8]   D.Y. Shang, B.X. Wang, "An extended study on steady-state laminar film condensation of a superheated vapour on an isothermal vertical plate," *International Journal of Heat and Mass Transfer,* vol. 40, no. 4, pp. 931-941, 1997.

[9]   S. Oh, S. T. Revankar, "Analysis of the complete condensation in a vertical tube passive condenser," *International Communications in Heat and Mass Transfer,* vol. 32, pp. 716-727, 2005.

[10] W.J. Minkowycz, E.M. Sparrow, "Condensation heat transfer in the presence of noncondensables, interfacial resistance, superheating, variable properties and diffusion," *International Journal of Heat and Mass Transfer,* vol. 9, pp. 1125-1144, 1966.

[11] C.Y. Wang, C.J. Tu, "Effects of noncondensable gas on laminar film condensation in a vertical tube," *International Journal of Heat and Mass Transfer,* vol. 32, no. 11, pp. 2339-2345, 1988.

[12] Yan W. M. and Lin T. F., "Combined heat and mass transfer in natural convection between vertical parallel plates with film evaporation," *International Jouranl of Heat and Mass Transfer,* vol. 33, pp. 529-541, 1990.

[13] J.L. Munoz-Cobo, L. Herranz, J. Sancho, I. Tkachenko, G. Verdu, "Turbulent vapor condensation with noncondensable gases in vertical tubes," *International Journal of Heat and Mass Transfer,* vol. 39, no. 15, pp. 3249-3260, 1996.

[14] N. K. Maheshwari, D. Saha, R.K. Sinha, M. Aritomi, "Investigation on condensation in presence of a noncondensable gas for a wide range of Reynolds number," *Nuclear Engineering and Design,* vol. 227, pp. 219-238, 2004.

[15] Z. Ait Hammou, B. Benhamou, N. Galanis, J. Orfi, "Laminar mixed convection of humid air in a vertical channel with evaporation or condensation at the wall," *International Journal of Thermal Sciences,* vol. 43, pp. 531-539, 2004.

[16] S. Oh, S. T. Revankar, "Experimental and theoretical investigation of film condensation with noncondensable gas," *International Journal of Heat and Mass Transfer,* vol. 49, pp. 2523-2534, 2006.

[17] M.K. Groff, S.J. Ormiston , H.M. Soliman, "Numerical solution of film condensation from turbulent flow of vapor–gas mixtures in vertical tubes," *International Journal of Heat and Mass Transfer,* vol. 50, pp. 3899-3912, 2007.

[18] V. Dharma Rao, V. Murali Krishna, K.V. Sharma, P.V.J. Mohana Rao, "Convective condensation of vapor in the presence of a noncondensable gas of high concentration in laminar flow in a vertical pipe," *Convective condensation of vapor in the presence of a nonconInternational Journal of Heat and Mass Transfer,* vol. 51, pp. 6090-6101, 2008.

[19] Li, Jun-De, "CFD simulation of water vapour condensation in the presence of noncondensable gas in vertical cylindrical condensers," *International Journal of Heat and Mass Transfer,* vol. 57, pp. 708-721, 2013.

[20] Mohamed Aboudou Kassim, Brahim Benhamou, Souad Harmand, "Effect of air humidity at the entrance on heat and mass transfers in a humidifier," *Applied Thermel Engineering,* vol. 31, pp. 1906-1914, 2001.

[21] Li, Jun-De, "CFD simulation of water vapour condensation in the presence of noncondensable gas in vertical cylindrical condensers," *International Journal of Heat and Mass Transfer 57 (2013) 708–721.,* vol. 57, pp. 708-721, 2013.

[22] Chanamon Chantana, S. Kumar, "Experimental and theoretical investigation of air-steam condensation in a vertical tube at low inlet steam fractions," *Applied Thermal Engineering,* vol. 54, pp. 399-412, 2013.

[23] F. Hassaninejadfarahani, M.K. Guyot, S.J. Ormiston, "Numerical analysis of mixed-convection laminar film condensation from high air mass fraction steam–air mixtures in vertical tubes," *International Journal of Heat and Mass Transfer,* vol. 78, pp. 170-180, 2014.

[24] Asis Giri, Dipanka Bhuyan, Biplab Das, "A study of mixed convection heat transfer with condensation from a parallel plate channel," *International Journal of Thermal Sciences,* vol. 98, pp. 165-178, 2015.

[25] Lin T. F., Chang C. G. et Yan W. M., "Analysis of combined buoyancy effects of thermal and mass diffusion on laminar forced convection heat transfer in a vertical tube," *Journal of Heat Transfer,* vol. 110, pp. 337-344, 1988.

[26] Debbissi C., Orfi J. et Ben Nasrallah S, "Evaporation of water by free convection in vertical channel including effects of wall radiative properties," *International Journal of Heat and Mass Transfer,* vol. 44, pp. 811-826, 2001.

[27] Siow E. C., Ormiston S. J et Soliman H.M., "A two-phase model for laminar film condensation from steam-air mixtures in vertical parallel-plate channels," *Inetrnational Journal of Heat and Mass Transfer,* vol. 40, pp. 365-375, 2004.

[28] Hubbard G. L., Denny V. E. et Mills A. F., "Droplet evaporation: effects of transients and variable properties," *Inetrnational Journal of Heat and Mass Transfer,* vol. 18, pp. 1003-1008, 1975.

[29] N., Chow L. C. et Chung J., "Evaporation of water into laminar stream of air and superheated steam," *International Journal of Heat and Mass Transfer,* vol. 26, pp. 373-380, 1983.

[30] Agunaoun A., Daif A et Daguenet M., "Évaporation en convection forcée d'un film mince s'écoulant en régime permanent, laminaire et sana onde, sur une surface plane inclinée," *International Journal of Heat and Mass Transfer,* vol. 37, no. 18, pp. 2947-2956, 1994.

[31] Gebhart B. and Pera L., "The nature of vertical natural convection flows resulting from the combined buoyancy effects of thermal and mass diffusion," *International Journal of Heat and Mass Transfer,* vol. 14, pp. 2025-2050, 1971.

[32] Aboudou Kassim Mohamed, *ÉTUDE NUMÉRIQUE ET EXPÉRIMENTALE DES TRANSFERTS COUPLÉS DE CHALEUR ET DE MASSE EN CONVECTION MIXTE DANS UN CANAL. Doctorate thesis in Energetics.Faculté des Sciences Semlalia-Marrakech, Morocco,* 2010.

[33] Yan W. M. et Soong C. Y., "Numerical study of liquid film cooling along an inclined plate.," *Wärme- und Stoffübertragung,* vol. 28, pp. 233-241, 1993.

[34] Yan W. M, "Mixed convection heat and masse transfer in rectangular ducts rotating about parallel axis," *Inetrnational Journal of Heat and Mass Transfer,* vol. 42, pp. 2955-2965, 1999.

[35] Lee K. T, Tsai H. L and Yan W. M, "Mixed convection heat and mass transfer in vertical rectangular ducts," *Int. J. Heat and Mass Transfer,* vol. 40, pp. 1621-1631, 1997.

[36] Patankar S.V, Numerical heat transfer in fluid flow, Hemisphere/ McGraw-Hill, New York, 1980.

[37] Shah R. K. et London A. L, Laminar flow forced convection in ducts, Academic Press,New York, USA, 1978.

[38] Bejan A, Convection heat transfer, John Wiley & Sons, Inc, 1984.

[39] Bruhhat, Simulation numérique de décollement instationnaire externe par une formule vitesse-pression:Application à l'écoulement autour d'un cylindre, Doctorate Thesis. I.N.P,Toulouse, 1968.

[40] Bailly M, "Thermodynamique technique", Bordas, 1973.

[41] Vachon M, « Étude de l'évaporation en convection naturelle », Doctorate Thesis.University of Poitiers, Poitiers, France., 1979.

[42] Debbissi C, Orfi J. and Ben Nasrallah S, " "Evaporation of water by free or mixed convection into humid air and superheated steam"," *Int. J. Heat and Mass Transfer,* vol. 46, pp. 4703-4715, 2003.

[43] Fujii T., Kato Y. and Bihara K., ""Expressions of transport and thermodynamic properties of air, steam and water"," Sei San Ka Gaku Ken Kuu Jo, Report no 66, Kyu Shu University, Kyu Shu, Japan., 1977.

Mr. HAMMOUDI Djamel was born on 07/12/1989 in Sidi Ali, Mostaganem. He held his Baccalaureate in Natural Sciences and Life in 2007 . He is a graduate of an engineering degree in petroleum production engineering, from the University of BOUMERDES (Ex- INH). He has been registrated in Magister at the Faculty of Mechanical Engineering and Engineering Processes, USTHB, Algiers since November 2013 in Mechanical Engineering, option: Mechanical Energy and Porous Media. His researches focus on petroleum production engineering and Heat and Mass transfer and phase change.

Abstract

In this work, we present a numerical solution of governing equations for steam condensation in vertical channel in the presence of a noncondensable gas for forced convection. A laminar downward flow of humid air circulates through the channel with a constant temperature and concentration and a uniform profile of velocity at the inlet. The one-third law is adopted to calculate the Thermo-physical properties in this study. The mathematical model solution is based on finite volume method and the pressure-velocity coupling is treated by SIMPLER Algorithm. Besides the transverse diffusion, the model includes the axial diffusion. The aim of this work is to carry out an investigation about the condensed flow rate. A wide range of inlet input parameters for the mixture of steam-air has been used to study the heat and mass transfer, where the condensed flow rate has been evaluated for different values of inlet parameters such us the temperature, the Reynolds number and the relative humidity as well as the aspect ratio. The obtained results show that the increase of inlet humidity, inlet Reynolds number and inlet temperature as well as the aspect ratio promotes condensation. The aforementioned parameters have the same effect on the released latent heat for condensation case.

Keywords : Condensation, noncondensable gas, thin liquid film, water vapor-air mixture, forced convection.

ملخص

الدراسة المتناولة في هذا البحث تقدم الحل الرقمي للمعادلات التي تحكم تكثيف البخار مع وجود غير مكثف في قناة عمودية في حالة الحمل الحراري القسري. تم تطبيق انسياب نزولي صفحي للهواء الرطب داخل القناة مع درجة حرارة, تركيز و سرعة ثابتين عند المدخل. قمنا باستخدام قاعدة الثلث المنتهية مع معالجة اقتران سرعة-ضغط بواسطة لحساب الخصائص الفيزيوحرارية. يستند حل النموذج الرياضي المستعمل على طريقة الأحجام خوارزمية SIMPLER. بالإضافة إلى الإنتشار العرضي, فإن النموذج يتضمن الإنتشار المحوري. الهدف من هذه الدراسة هو حساب التدفق المتكثف. وقد تم استخدام مجموعة واسعة من المقاييس عند مدخل القناة من أجل دراسة الإنتقال الحراري و الكتلي أين تم تقييم التدفق المتكثف بدلالة درجة الحرارة, عدد رينولدز و الرطوبة النسبية عند المدخل بالإضافة إلى عامل الشكل. أظهرت النتائج أن زيادة الرطوبة النسبية, عدد رينولدز و درجة الحرارة عند مدخل القناة بالإضافة إلى عامل الشكل تحسن التكثيف. هذه المعايير لها نفس التأثير على الحرارة الكامنة المتحررة في حالة التكثيف.

كلمات مفتاحيةً: تكثيف، غاز غير مكثف، غشاء سائل رقيق، خليط بخار-غاز، حمل حراري قسري

Résumé

Dans ce travail, on présente une résolution numérique des équations gouvernantes pour la condensation d'une vapeur en présence d'un incondensable dans un canal vertical pour le cas de convection forcée. Un écoulement d'air humide laminaire descendant circule dans le canal avec une température, une concentration constantes et un profil de vitesse uniforme à l'entrée. La loi de tiers est adoptée pour calculer les propriétés thermo-physiques. La résolution du modèle mathématique est basée sur la méthode des volumes finis et le couplage vitesse-pression est traité par l'algorithme SIMPLER. En outre de la diffusion transversale, le model inclus la diffusion axial. L'objective de ce travail est d'effectuer une investigation sur le débit condensé. Une large gamme des paramètres d'entrée a été utilisée pour étudier le transfert de chaleur et de masse où le débit condensé a été évalué en fonction des paramètres d'entré tel-que la température, le nombre de Reynolds et l'humidité relative et aussi le facteur de forme. Les résultats obtenus montrent que l'augmentation de l'humidité relative, le nombre de Reynolds et la température à l'entrée du canal et aussi le facteur de forme améliore la condensation. Ces paramètres ont le même effet sur la chaleur latente libérée pour le cas de condensation.

Mots clés : Condensation, gaz incondensable, film liquide mince, mélange vapeur-air, convection forcée.